iScience

CellPress
OPEN ACCESS

Article

Rebalance of mitophagy by inhibiting LRRK2 improves colon alterations in an MPTP *in vivo* model

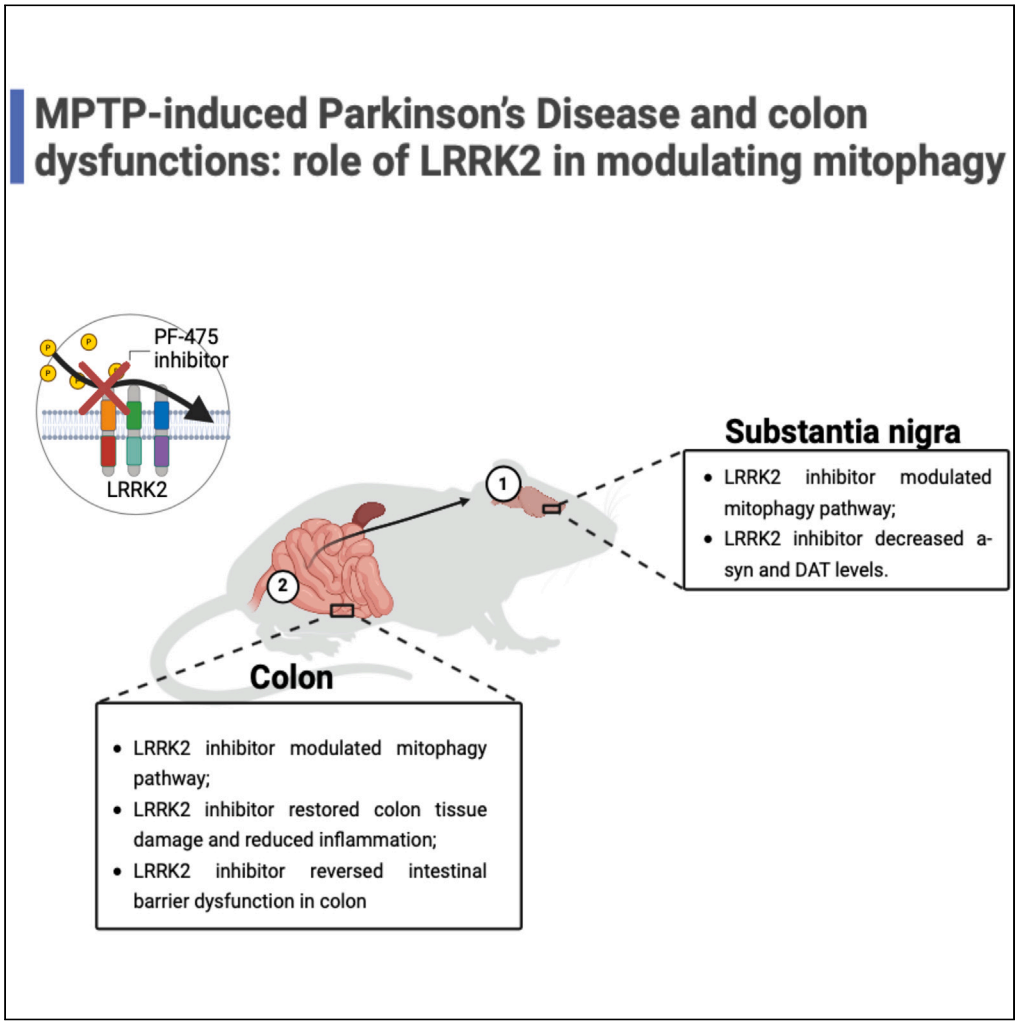

Alessia Filippone, Deborah Mannino, Laura Cucinotta, Fabrizio Calapai, Lelio Crupi, Irene Paterniti, Emanuela Esposito

eesposito@unime.it

Highlights

LRRK2 inhibitor demonstrated neuroprotection in a mouse model of MPTP-induced PD

LRRK2 inhibitor reduced pro-inflammatory markers and modulated mitophagy pathway

LRRK2 inhibitor modulated colon damage associated with PD

LRRK2 inhibitor improves colon barrier and integrity during PD

Filippone et al., iScience 27, 110980
October 18, 2024
https://doi.org/10.1016/j.isci.2024.110980

iScience

CellPress
OPEN ACCESS

Article

Rebalance of mitophagy by inhibiting LRRK2 improves colon alterations in an MPTP *in vivo* model

Alessia Filippone,[1] Deborah Mannino,[1] Laura Cucinotta,[1] Fabrizio Calapai,[2] Lelio Crupi,[1] Irene Paterniti,[1] and Emanuela Esposito[1,3,*]

SUMMARY

Mutations in the leucine-rich repeat kinase 2 (LRRK2) gene are common genetic causes of Parkinson's disease (PD). Studies demonstrated that variants in LRRK2 genetically link intestinal disorders to PD. We aimed to evaluate whether the selective inhibitor of LRRK2, PF-06447475 (PF-475), attenuates the PD induced by 1-methyl-4-phenyl-1,2,3,6-tetrahydropyridine (MPTP) in central nervous system (CNS) and in the gastrointestinal system. CD1 mice received four intraperitoneal injections of MPTP (20 mg/kg, total dose of 80 mg/kg) at 2 h intervals (day 1). After 24 h PF-475 was administered intraperitoneally at the doses of 2.5, 5, and 10 mg/kg for seven days. LRRK2 inhibition reduced brain α-synuclein and modulated mitophagy pathway and reduced pro-inflammatory markers and α-synuclein aggregates in colonic tissues through the modulation of mitophagy proteins. LRRK2 inhibition suppressed MPTP-induced enteric dopaminergic neuronal injury and protected tight junction in the colon. Results suggested that PF-475 may attenuate gastrointestinal dysfunction associated to PD.

INTRODUCTION

One of the most common chronic neurodegenerative diseases, known as Parkinson's disease (PD), affects 1% of adults older than 60 years and appear as distinctive motor symptoms such as resting tremor, bradykinesia, muscle rigidity, and postural balance disorders and nonmotor symptoms, like cognitive decline, depression, and anxiety. Symptomatology is rightly correlated to an abnormal accumulation of Lewy bodies (LBs), defined as neuroaxonal spheroids with a dense core largely containing α-synuclein and a loss of neurons in substantia nigra pars compacta (SNpc).[1] Moreover, it has been proposed that gastrointestinal tract might be the site of initiation of PD or vice versa, suggesting that not only the central nervous system (CNS) is impaired from motor and nonmotor symptoms, also the gastrointestinal system may take an active part in the pathophysiological changes PD-related and that results in a compromission of colon functionality surrounded by misfolded α-synuclein.[2] In order to treat PD, dopamine drug therapy and brain surgical electrical stimulation are currently the most common clinical treatments for symptomatic conditions. However, these methods can only improve PD symptoms and cannot stop the disease from getting worse also outside the brain for instance throughout the gastrointestinal system. Thus, it is necessary to investigate alternative effective approaches that can not only improve motor and nonmotor symptoms but also attenuate the accumulation of misfolded α-synuclein in CNS and gastrointestinal system both.[3] Indeed, α-synuclein deposition occurs in the myenteric and submucosal plexuses and mucosal nerve fibers of PD subjects, with a clear deposition throughout the entire enteric nervous system (ENS). In several number of PD cases, it has been found specific mutation in genes of various functions including PINK1, Parkin, α-synuclein, and also leucine repeat kinase 2 (LRRK2). LRRK2 is a 286 kDa multidomain protein belonging to the Roco family of G-proteins. Its structure consists of N-terminal armadillo, ankyrin, and LRR repeats followed by a small GTPase like domain called Roc (Ras of complex proteins), a COR (C-terminal of Roc), a kinase, and a WD40 domain. Particularly, linked mutations to LRRK2 gains its kinase activity contributing to the α-synuclein propagation and aggregation in SNpc and in gastrointestinal system.[4] As such, LRRK2 inhibitors have been reported as tools to pharmacologically and structurally inhibit kinase activity and to cross the brain blood barrier (BBB) driving diverse signaling pathways and repairing cellular processes such as cytoskeleton remodeling, adequate vesicular trafficking, functional control of autophagy, and mitochondria.[5–8] Furthermore, recently studies performed on microRNAs (miRNAs) have discovered that some of these could play an important role by modulating LRRK2. In particular, MiR-185 was found to have a neuroprotective effect by negatively targeting LRRK2.[9] Mitochondrial dysfunctions have been reported in the pathogenesis of both sporadic PD and familial Parkinsonism with a reduction of its dynamics about 40% in the SNpc of 1-methyl-4-phenyl-1,2,3,6-tetrahydropyridine (MPTP)-induced mice and PD patients. Indeed, the highly controlled fission/fusion process of misfolded proteins and organelles that occur in mitochondria

[1]Department of Chemical, Biological, Pharmaceutical and Environmental Sciences, University of Messina, Viale Ferdinando Stagno D'Alcontres, 31-98166 Messina, Italy
[2]Department of Clinical and Experimental Medicine, University of Messina, 98125 Messina, Italy
[3]Lead contact
*Correspondence: eesposito@unime.it
https://doi.org/10.1016/j.isci.2024.110980

results defective in PD because of the presence of an extensive damage to mitochondrial segments that cannot be repaired for local repair mechanism and thus undergo recycling through autophagy and lysosome system (ALS).[10] Therefore, mitochondrial dysfunction appears to be a central pathogenic mechanism implicated in PD. Mitochondrial dysfunction is highly involved in α-synuclein aggregation, neuroinflammation, and the accumulation of oxidative stress. Today the consequences of mitochondrial dysfunction have been overcome by using antioxidants and NAD+ supplements such as nicotinic acid. However, further research is needed to investigate the involvement of mitochondrial dysfunction in PD as this could represent a potential therapeutic target.[11] Within this perspective, under physiological conditions, the kinase activity of LRRK2 mediates mitochondrial fission and maintains a balanced autophagic flux by interfering with the cellular localization of lysosomes. Furthermore, LRRK2 forms a complex with mitochondrial membrane proteins initiating mitophagy. In PD, mutated LRRK2 elongates the mitochondrial network and leads to poor degradation of malfunctioning mitochondria. *In vitro* studies showed that the treatment with LRRK2 type II inhibitors stabilizes an open conformation of the catalytic domain of LRRK2, improving the motility of kinesin and dynein, two motor proteins that drive mitochondrial transport.[12] The mitochondrial quality control failure implicates misfolded proteins and organelles to being degraded from ALS that became engulfed and non-stop recruit autophagy selective activators like microtubule associated protein 1 light chain 3 (MAP-LC3), optineurin, and nuclear factor kappa B subunit (NF-κB) to form autolysosomes and ultimately degrade cargos.[13] In this context, it is still unclear how LRRK2 or its inhibition could contribute to mitochondrial dysfunction in PD and in the gastrointestinal system. Here, we aimed to evaluate the mechanism of action of LRRK2 in modulating molecular signaling at the mitochondrial level and ALS systems in an *in vivo* model of MPTP induced PD by preventing CNS neurodegeneration and pathological related consequences to the gastrointestinal system.

RESULTS

In vitro results

PF-475 reduced p-LRRK2 levels in vitro

To corroborate how PF-475 could regulate LRRK2 expression *in vitro*, we used differentiated SHSY5Y cells and stimulated them with MPTP (3 mM) for 2 h after pretreatment with PF-475 (1 and 3 μM). Then, cell lysates were used to perform western blot analysis. Cells stimulated with MPTP showed elevated levels of *p*-Ser 935 compared to control cells. Conversely, treatments with PF-475 in a concentration-dependent manner significantly reduced *p*-Ser 935 compared to cells stimulated with MPTP (Figure S1A, see densitometric analysis A1). These *in vitro* data confirm that PF-475 negatively regulates LRRK2 phosphorylation, accordingly with previous studies.[14,15]

In vivo results

Tissue preparation

24 h after MPTP injection, animals received intraperitoneal administration of PF-475 at doses of 2.5 mg/kg, 5 mg/kg, and 10 mg/kg, respectively, once daily for up to 7 days. On the eighth day the animals were sacrificed, and the colon and brain were surgically isolated. For molecular biology analyzes such as western blot and ELISA assay, brain and colon were collected and processed to perform protein extraction. For measurement of dopamine, DOPAC, and homovanilic acid (HVA) levels, the striatum was removed and processed for high-performance liquid chromatography (HPLC) analysis. For histological analyses, colon and brain tissues were fixed in 10% (w/v) PBS-buffered formaldehyde solution at 25°C for 24 h. After a dehydration process through a scale with increasing concentrations of alcohols and xylene, the tissues were embedded in paraffin and subsequently cut with a microtome obtaining 7 μm thick sections to perform the following analyses: histological evaluation, immunohistochemical analysis, and immunofluorescence analysis.

LRRK2 inhibition reduced α-syn aggregates and prevented dopamine depletion after MPTP intoxication in mouse brain tissue

We performed immunoblot analysis on the brain protein extract of mice from each experimental group to demonstrate the selective inhibition of LRRK2 following PF-475 treatment. We evaluated relative proportion of LRRK2 phosphorylation *p*-LRRK2 on Ser935 as well as total LRRK2 levels. As expected, *p*-LRRK2 Ser935 was significantly higher in brain tissues of MPTP-injected mice compared to control mice, while intraperitoneal treatment with PF-475 at the highest doses of 5 mg/kg and 10 mg/kg significantly reduced *p*-LRRK2 Ser935 compared with MPTP-injected mice (Figure 1A, see densitometric analysis A1). In contrast, intraperitoneal treatment with PF-475 at the lowest dose of 2.5 mg/kg was unable to downregulate *p*-LRRK2 Ser935 in the brain of MPTP-injected mice (Figure 1A, see densitometric analysis A1; $p = 0.68$; $F(4,45) = 0.572$, one-way ANOVA method, followed by Bonferroni post hoc test for multiple comparisons). To further investigate the effects of PF-475 on LRRK2 kinase activity in the brain we assessed the levels of the downstream protein *p*-Rab12 by western blot analysis (Figure S1B, see densitometric analysis B1). Data demonstrated that *p*-Rab12 brain levels were significantly higher in MPTP mice compared to control mice. Intraperitoneal treatment with PF-475 at doses of 5 mg/kg and 10 mg/kg reduced the levels of this downstream protein compared to MPTP mice confirming a significant reduction in LRRK2 signaling. Moreover, since the accumulation of α-syn in dopaminergic neurons is a critical marker of PD, we wanted to evaluate the expression of this protein to confirm the key role of LRRK2 in the neurodegenerative process and that its inhibition represents a potential therapeutic target for the treatment of the PD. Quantitative western blot analysis of whole native gel band from brain samples revealed decreased α-Syn tetramers and monomers following PF-475 treatment at the highest doses of 5 mg/kg and 10 mg/kg compared to MPTP-injected mice (Figures 1B and C, see densitometric analysis B1 and C1, respectively). Consistently, whole native gel densitometric analysis (Figure 1 D; $p = 0.52$; $F(4,45) = 0.824$, one-way ANOVA method, followed by Bonferroni

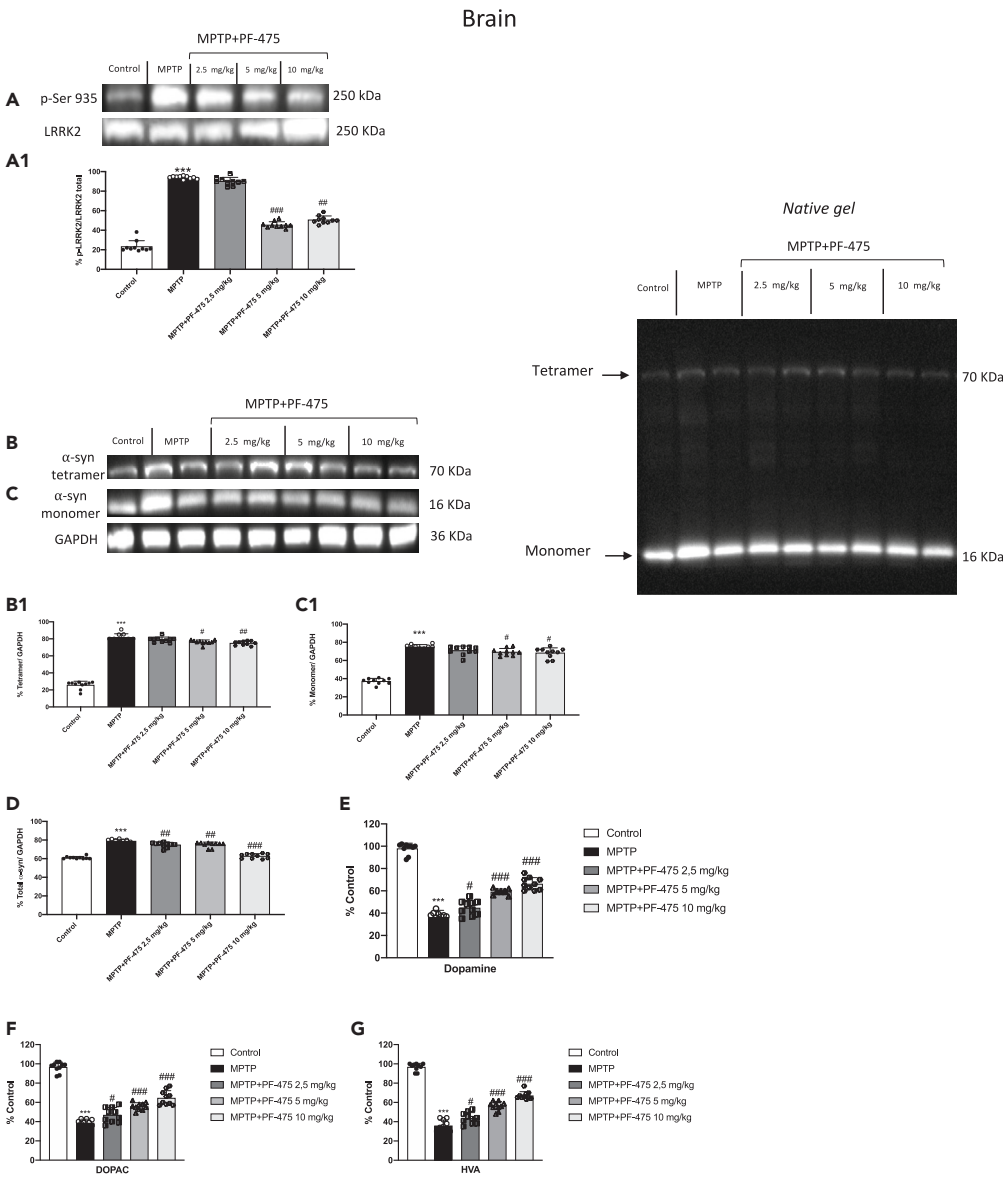

Figure 1. Effect of LRRK2 inhibition on α-syn aggregates and dopamine in mouse brain

Representative western blot of phosphorylated LRRK2 at Serine 935 protein expression level in cytosolic fraction of brain tissues after MPTP intoxication and PF-475 treatments (one-way ANOVA method, followed by Bonferroni post hoc test for multiple comparisons $p = 0.68$; $F(4,45) = 0.572$) (A, see densitometric analysis A1). Representative western blot of α-syn tetramer and monomer protein expression level in brain tissues after MPTP intoxication and PF-475 treatments (B and C; see densitometric analysis B1, C1, respectively). Total densitometric analysis of α-Syn monomers and tetramers (one-way ANOVA method, followed by Bonferroni post hoc test for multiple comparisons $p = 0.52$; $F(4,45) = 0.824$) (D). MPTP-injected animals exhibited a considerable loss of dopamine (one-way ANOVA method, followed by Bonferroni post hoc test for multiple comparisons $p = 0.18$; $F(4,45) = 1.66$) (E), and its metabolites DOPAC (one-way ANOVA method, followed by Bonferroni post hoc test for multiple comparisons, $p = 0.02$; $F(4,45) = 3.39$) (F) and HVA (one-way ANOVA method, followed by Bonferroni post hoc test for multiple comparisons, $p = 0.44$; $F(4,45) = 0.965$) (G) compared to the control mice; contrarily, treatment with PF-475 in a dose-dependent manner 2.5 mg/kg, 5 mg/kg and 10 mg/kg increased metabolites levels (E–G). Data are representative of at least three independent experiments. Values are means ± SD. Distribution of values come from individual animals. One-way ANOVA test. ***$p < 0.001$ vs. control; #$p < 0.05$ vs. MPTP; ##$p < 0.01$ vs. MPTP; ###$p < 0.001$ vs. MPTP.

post hoc test for multiple comparisons) showed a significant increase of α-syn aggregates in brain samples of MPTP-injected mice compared to control mice, while a dose-dependent reduction of total α-syn aggregates was observed in mice treated with PF-475 at doses of 2.5 mg/kg, 5 mg/kg and 10 mg/kg compared to MPTP-injected mice. As shown in Figure 1 whole native gel band levels were standardized to GAPDH levels as an internal control. Immunohistochemical analysis of midbrain sections confirmed significant accumulation of α-syn in

MPTP-damaged mice (Figure S1D, objective 40× D1) compared to control mice (Figure S1C, objective 40× C1). Furthermore, our results showed that the lowest dose, PF-475 (2.5 mg/kg) (Figure S1E, objective 40× E1) was unable to significantly counteract synuclein aggregates compared to MPTP-injected mice. Differently, the doses of 5 mg/kg and 10 mg/kg showed a greater reduction in α-syn deposition when compared to MPTP mice (Figures S1F and S1G, objective 40× F1 and G1, respectively, see score H). Degeneration of the nigrostriatal innervation leads to dopaminergic cell loss which is a typical feature of the pathogenesis of PD. Our results confirmed the neuroprotective role of the LRRK2 antagonist, PF-475, by evaluating striatal levels of dopamine and its metabolites such as 3,4-dihydroxyphenylacetic acid (DOPAC) and HVA. MPTP intoxication significantly reduced striatal dopamine (Figure 1E; $p = 0.18$; $F(4,45) = 1.66$, one-way ANOVA method, followed by Bonferroni post hoc test for multiple comparisons), DOPAC (Figure 1F; $p = 0.02$; $F(4,45) = 3.39$, one-way ANOVA method, followed by Bonferroni post hoc test for multiple comparisons) and HVA levels (Figure 1G; $p = 0.44$; $F(4,45) = 0.965$, one-way ANOVA method, followed by Bonferroni post hoc test for multiple comparisons) compared to control mice. Treatment with PF-475 at doses of 2.5 mg/kg, 5 mg/kg, and 10 mg/kg showed a partial recovery of the levels of dopamine and its metabolites in a dose-dependent manner. In addition, we confirmed DAT expression in brain sections by immunohistochemical analysis. The results obtained demonstrated a significant loss of DAT-positive staining in MPTP-injected mice (Figure S1I, objective 40× I1) compared to control mice (Figure S1I, objective 40× I1). The recovery of DAT levels was notable after administration of PF-475 at the dose of 5 mg/kg and most effective at the dose of 10 mg/kg (Figures S1L and S1M, objective 40× L1 and M1, respectively), compared to the MPTP group. In contrast, the lowest dose of PF-475 (2.5 mg/kg) (Figure S1K, objective 40× K1), did not significantly enhance DAT expression (see score N). Collectively, these results supported the neuroprotective capabilities of the LRRK2 selective inhibitor, PF-475 in a mouse model of MPTP-induced nigrostriatal degeneration.

LRRK2 inhibition modulated mitophagy pathway in brain tissue

LRRK2 mutations involved in the pathogenesis of PD lead to an increase in its kinase activity.[16,17] Increased kinase activity of LRRK2 reduces the interaction between the optineurin autophagy receptor (OPT) with ubiquitous mitochondrial outer membrane (OMM) proteins resulting in a negative impact on mitophagy.[18] Indeed, OPT plays a key role in mitophagy not only targeting dysfunctional mitochondria to autophagosomal membranes, but also facilitating the formation of autophagosomal membrane.[19] Our results demonstrated that MPTP-injected mice showed a compromised mitophagy demonstrating low levels of OPT compared to control mice. PF-475 treatment significantly affected the mitophagy pathway through the significant increase of OPT expression compared to MPTP-injected mice (Figure 2A, see densitometric analysis A1; $p = 0.09$; $F(4,45) = 2.16$, one-way ANOVA method, followed by Bonferroni post hoc test for multiple comparisons). The process of mitophagy is modulated by other different proteins including LAMP2 and p62. LAMP2, a lysosomal membrane protein, plays an important role in lysosomal stability as well as in autophagy. In addition, it has recently been demonstrated that disruption of lysosomal function, due to altered LAMP2 activity can lead to the accumulation of damaged cellular components and an increase in oxidative stress.[20] The overexpression of LAMP2 increases autophagy activity, and this effect is accompanied by decreased levels of p62.[21] As shown in Figure 2 we found that LAMP2 expression in MPTP-injected mice was significantly reduced compared to control mice (Figure 2B, densitometric analysis B1; $p = 0.04$; $F(4,45) = 2.77$, one-way ANOVA method, followed by Bonferroni post hoc test for multiple comparisons), conversely, p62 expression was significantly increased in MPTP-injected mice compared with control mice (Figure 2C, densitometric analysis C1; $p = 0.11$; $F(4,45) = 2.02$, one-way ANOVA method, followed by Bonferroni post hoc test for multiple comparisons). However, treatments with PF-475 at the doses of 5 mg/kg and 10 mg/kg significantly increased LAMP2 expression compared to MPTP mouse. On the other side, a significant reduction of p62 following PF-475 treatment at the doses of 2.5 mg/kg, 5 mg/kg, and 10 mg/kg was observed compared with the MPTP group (Figure 2C, see densitometric analysis C1). These data could indicate a restoration of increased autophagic flux in brain tissue following PF-475 treatment. In addition, impaired autophagic flux increases pro-inflammatory mediators such as tumor necrosis factor-α (TNF-α), which is highly toxic to dopaminergic neurons and a major mediator of neuroinflammation in PD.[22] Our results demonstrated an increased expression of the pro-inflammatory cytokine TNF-α in MPTP-injected mice compared with control mice. In contrast, treatment with PF-475 significantly reduced TNF-α expression levels at doses of 5 mg/kg and 10 mg/kg compared to MPTP-injected mice (Figure 2D, see score D1; $p = 0.16$; $F(4,45) = 1.86$, one-way ANOVA method, followed by Bonferroni post hoc test for multiple comparisons). Also, to further investigate the effects of PF-475 on mitolysosome formation, we performed immunofluorescence analysis of LAMP2 in brain tissues. LAMP2 represents an important lysomal marker highly expressed during mitochondrial degradation.[23,24] In our hands, treatments with PF-475 at doses of 5 mg/kg and 10 mg/kg significantly increased the number of lysosomes positive for LAMP2 staining when compared to MPTP mice (Figures S3A–S3E, insets A1 to E1, see score F). Moreover, to evaluate mitochondrial function we measured ATP and lipid peroxidation levels by MDA assay, in brain tissues. Mitochondria are the powerhouses of cells and are the main source of ATP. Impaired mitochondrial function is closely related to reduced ATP levels, as well as abnormal mitochondrial dynamics such as reduced mitochondrial biogenesis and imbalanced fusion and fission.[25–27] Furthermore, levels of MDA, a by-product of lipid peroxidation, accumulate due to mitochondrial dysfunction.[28,29] Our results showed that the brain of MPTP mice exhibited mitochondrial dysfunction revealed by increased MDA levels and decreased ATP levels compared to control mice (Figures S4A and S4B). However, improved mitochondrial function was observed following treatment with PF-475 at doses of 5 mg/kg and 10 mg/kg as indicated by a significant increase in ATP levels and a decrease in MDA production.

LRRK2 inhibition ameliorated colon damage in MPTP-injected mouse

We also evaluated the relative proportion of LRRK2 phosphorylation *p*-LRRK2 on Ser935 as well as total LRRK2 levels in colon samples. Study of LRRK2 phosphorylation at Ser-935 expression in colonic tissues of MPTP-treated mouse demonstrated overexpression of this

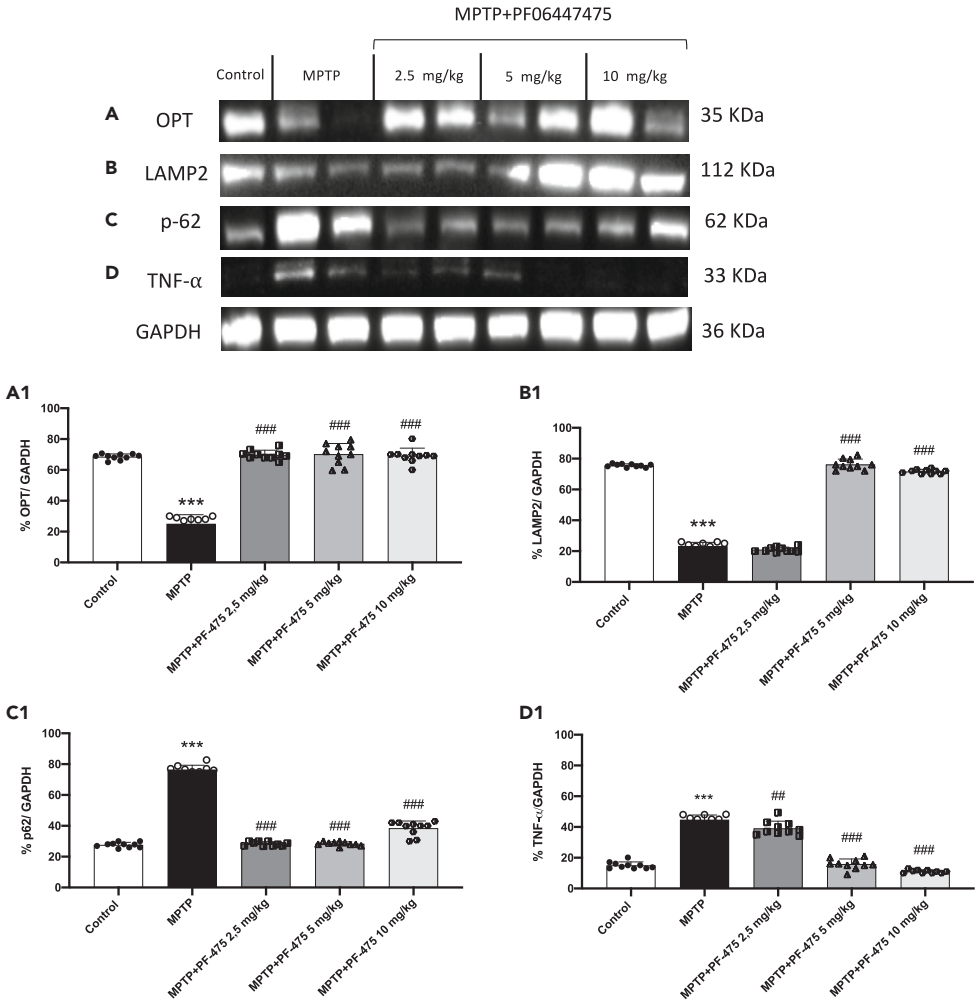

Figure 2. Effect of LRRK2 inhibition on mitophagy pathway in brain

Cytosolic protein fractions of brain tissues were used to evaluate mitophagic protein expression such as OPT, LAMP2, and p62 and pro-inflammatory cytokine TNF-α after MPTP intoxication and PF-475 treatments. Representative western blot of mitophagic protein are shown (A; $p = 0.09$; F(4,45) = 2.16, one-way ANOVA method, followed by Bonferroni post hoc test for multiple comparisons), (B; $p = 0.04$; F (4,45) = 2.77, one-way ANOVA method, followed by Bonferroni post hoc test for multiple comparisons) and (C; $p = 0.11$; F(4,45) = 2.02, one-way ANOVA method, followed by Bonferroni post hoc test for multiple comparisons), see densitometric analysis (A1, B1 and C1, respectively). Western blot of pro-inflammatory cytokine TNF-α are shown (D; $p = 0.16$; F(4,45) = 1.86, one-way ANOVA method, followed by Bonferroni post hoc test for multiple comparisons), see densitometric analysis (D1). Data are representative of at least three independent experiments. Values are means ± SD. Distribution of values come from individual animals. One-way ANOVA test. ***$p < 0.001$ vs. control; ##$p < 0.01$ vs. MPTP; ###$p < 0.001$ vs. MPTP.

protein kinase after MPTP intoxication compared to control animals (Figure 3A, see densitometric analysis A1). Intraperitoneal treatment with PF-475 in a dose-dependent manner significantly reduced *p*-LRRK2 Ser935 (Figure 3A, see densitometric analysis A1; $p = 0.4$; F(4,45) = 2.84, one-way ANOVA method, followed by Bonferroni post hoc test for multiple comparisons). In addition, the levels of LRRK2 downstream protein *p*-Rab10 were significantly reduced following treatment with PF-475 at doses of 5 mg/kg and 10 mg/kg compared to MPTP mice (Figure S2A, see densitometric analysis A1). Furthermore, the MPTP group showed more severe colonic inflammation, loss of crypt architecture, edema, and the extent of infiltration with inflammatory cells damage extending in the submucosa (Figure 3C, objective lens 20× C1) layers than the control group (Figure 3B, objective lens 20× B1). Instead, treatment with PF-475 at the highest doses of 5 mg/kg (Figure 3E, objective lens 20× E1) and 10 mg/kg (Figure 3F, objective lens 20× F1) significantly improved tissue architecture and reduced inflammation compared to MPTP mouse. Instead, no significant difference was found following treatment with PF-475 at the lower dose of 2.5 mg/kg in reducing the histological score (Figure 3D, objective lens 20× D1, score G; p = <0.001.; F(4,45) = 6.38, one-way ANOVA method, followed by Bonferroni post hoc test for multiple comparisons). Taken together, these results suggested for the first time, an involvement of LRRK2 in MPTP-induced intestinal damage and demonstrated how selective inhibition of LRRK2 through PF-475 administration could restore colonic damage in MPTP mice.

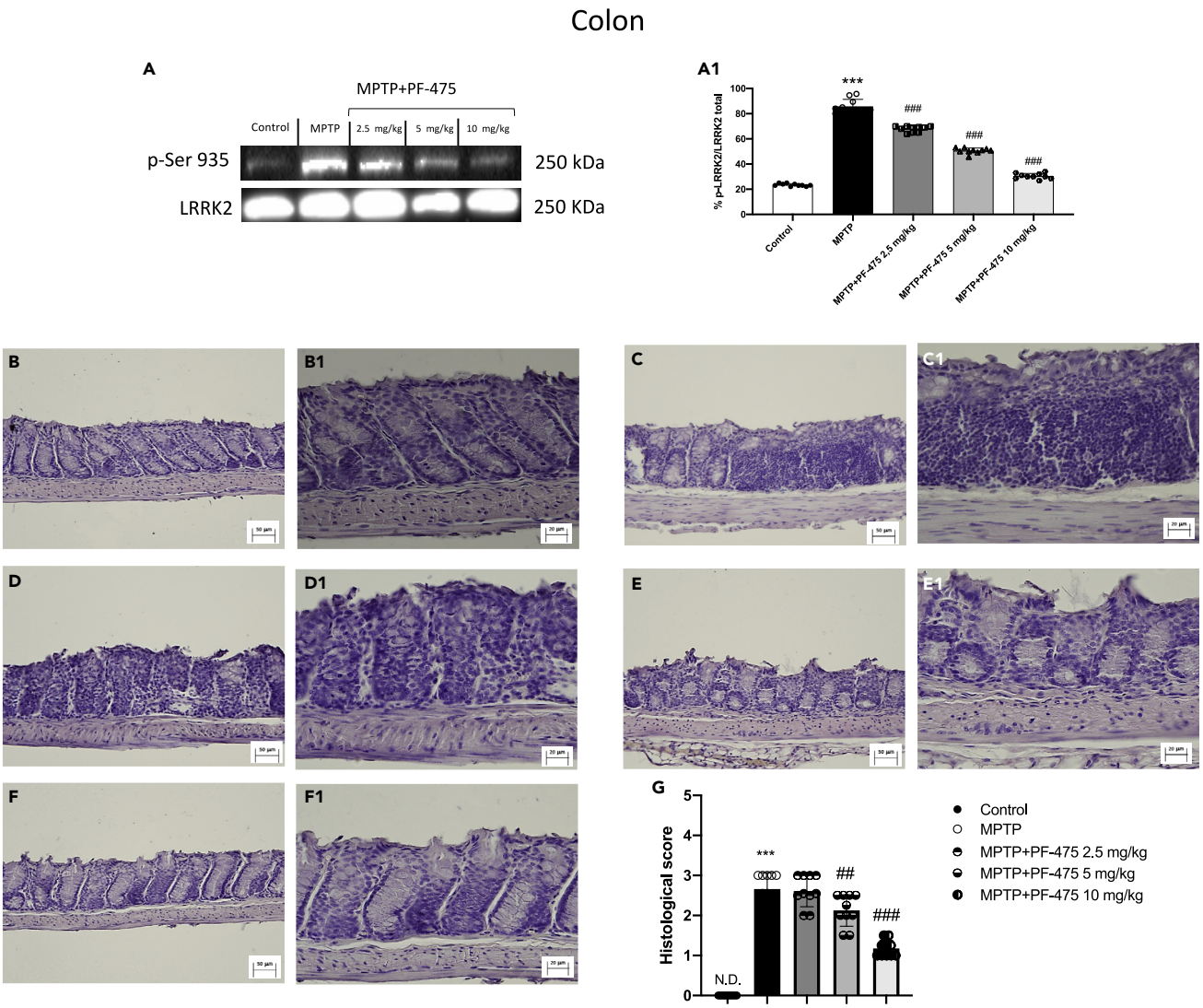

Figure 3. Effects of PF-475 treatments on histological damage in MPTP-injected mouse colon

Representative Western blot of phosphorylated LRRK2 at Serine 935 protein expression level in cytosolic fraction of colon tissues after MPTP and PF-475 treatments (A, densitometric analysis A1; $p = 0.4$; $F(4,45) = 2.84$, one-way ANOVA method, followed by Bonferroni post hoc test for multiple comparisons). Hematoxylin and eosin staining of control group (B, B1), MPTP group (C, C1), PF-475 2.5 mg/kg treatments after MPTP (D, D1), PF-475 5 mg/kg treatments after MPTP (E, E1) and PF-475 10 mg/kg treatments after MPTP (F, F1), see histological score (G; $p = <0.001$.; $F(4,45) = 6.38$, one-way ANOVA method, followed by Bonferroni post hoc test for multiple comparisons). Data are representative of at least three independent experiments. Values are means ± SD. Distribution of values come from individual animals. One-way ANOVA test. ***$p < 0.001$ vs. control; ##$p < 0.01$ vs. MPTP; ###$p < 0.001$ vs. MPTP.

Effect of PF-475 on pro-inflammatory response in colon tissues

In parallel with CNS inflammation during PD, recent studies indicate similar processes at peripheral sites.[30] In particular, increases in proinflammatory markers levels in the colon provide strong evidence of gastrointestinal inflammation in patients with PD.[31] Moreover, previous studies have reported that the PD model induced by MPTP reflects an inflammatory response in the colon very similar to the gastrointestinal conditions of PD patients.[32,33] Therefore, we used western blot analysis and ELISA assay to evaluate the effects of PF-475 on the inflammatory markers in the colon tissues following MPTP intoxication. The results showed that, in MPTP mouse, the expression of pro-inflammatory enzymes such as inducible nitric oxide synthase (iNOS) and COX-2 in colon tissues increased significantly compared to control animals (Figures 4A and 4B, see densitometric analysis A1 and B1, respectively; $p = 0.005$, $F(4,45) = 4.25$ for iNOS and $p = 0.07$, $F(4,45) = 2.31$ for COX-2, one-way ANOVA method, followed by Bonferroni post hoc test for multiple comparisons). Following intraperitoneal treatment with PF-475 at doses of 2.5 mg/kg, 5 mg/kg, and 10 mg/kg a significant reduction of these pro-inflammatory markers was observed compared to MPTP-injected animals, in a dose-dependent manner. Furthermore, ELISA assay revealed that IL-1β concentration increased in the colon of MPTP mice compared to control animals, while PF-475 treatment was able to partially reduce, in a dose-dependent manner, the levels of the

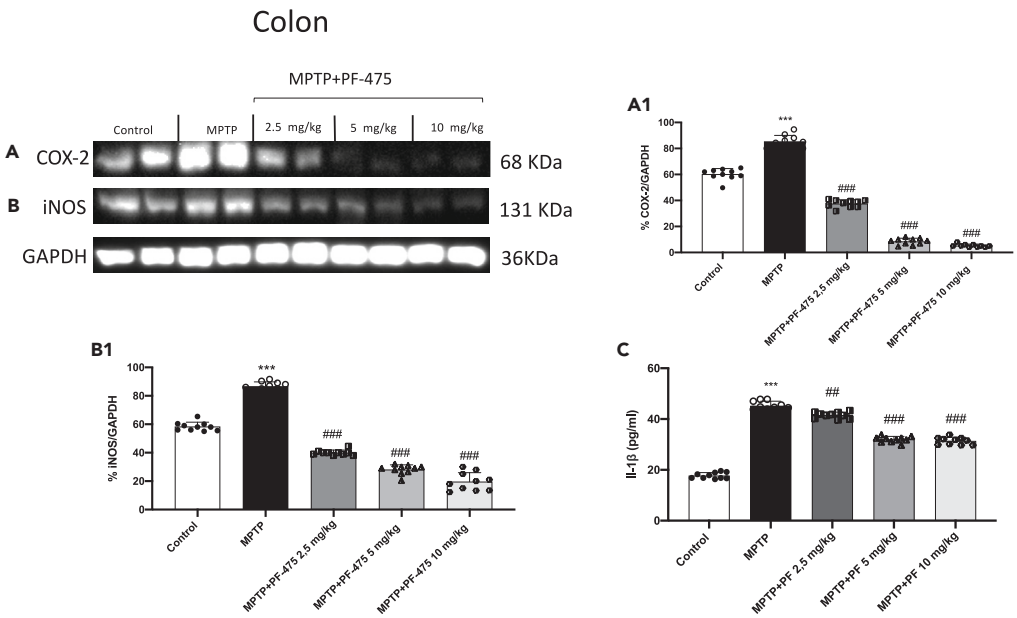

Figure 4. Effect of PF-475 on pro-inflammatory response induced by MPTP intoxication in colon tissues

Representative western blot of pro-inflammatory enzyme iNOS and COX-2 in cytosolic fraction of colon tissues after MPTP and PF-475 treatments (A; $p = 0.005$, $F(4,45) = 4.25$, one-way ANOVA method, followed by Bonferroni post hoc test for multiple comparisons) (B; $p = 0.07$, $F(4,45) = 2.31$, one-way ANOVA method, followed by Bonferroni post hoc test for multiple comparisons), see densitometric analysis (A1, B1, respectively). ELISA method was performed for detection of IL-1β in cytosolic fraction of colon tissues (C). Data are representative of at least three independent experiments. Values are means ± SD. Distribution of values come from individual animals. One-way ANOVA test. *$p < 0.05$ vs. control ***$p < 0.001$ vs. control; ##$p < 0.01$ vs. MPTP; ###$p < 0.001$ vs. MPTP.

pro-inflammatory cytokine compared with MPTP mice (Figure 4C). In summary, these results suggest that administration of the selective LRRK2 antagonist showed high efficacy in reducing the levels of proinflammatory markers in colon tissues in mice with MPTP-induced PD.

PF-475 reduced α-synuclein accumulation in the colon of MPTP mice

It has been reported that during PD, colonic dysfunction associated with dopaminergic degeneration in the ENS is closely related to an increase in α-synuclein, which is found in the colon of PD patients.[34] In our study, through immunohistochemical analysis, we estimated the number of α-synuclein-positive enteric cells in the colon of MPTP-injected mice to evaluate whether PF-475 could reduce its accumulation. In our study, through immunohistochemical analysis, we estimated the number of α-synuclein-positive enteric cells in the colon of MPTP-injected mice to evaluate whether PF-475 could reduce its accumulation. The results showed that MPTP injection (Figure 5B, objective lens 20× B1, see score F) led to an increase of α-synuclein in the colonic submucosa compared to control animals (Figure 5A, objective lens 20× A1, see score F). Therefore, in line with other studies, MPTP induced intestinal damage accompanied by the accumulation of α-syn in the colon[35,36] and that is closely related to the gastrointestinal non-motor symptoms of PD. Moreover, our results, demonstrated that PF-475 at the dose of 5 mg/kg (Figure 5C, objective lens 20× C1, see score F) and 10 mg/kg (Figure 5D, objective lens 20× D1, see score F; $p = 0.4$; $F(4,45) = 2.84$, one-way ANOVA method, followed by Bonferroni post hoc test for multiple comparisons) protected colon tissue from MPTP by significantly reducing the number of α-synuclein positive cells compared to MPTP mice. In addition, the result was confirmed by western blot analysis which revealed an accumulation of different forms of α-syn, including tetrameric (Figure 5G, see densitometric analysis G1) and monomeric (Figure 5H, see densitometric analysis H1) in the colon of mice MPTP injected versus control animals. Treatment with PF-475 significantly reduced α-synuclein tetramer at all doses compared to MPTP mice (Figure 5G, see densitometric analysis G1). Otherwise, PF-475 treatment reduced α-synuclein monomer at doses of 5 mg/kg and 10 mg/kg compared to MPTP mice. In each case the densitometric analysis of total α-synuclein (Figure 5I; $p = 0.001$; $F(4,45) = 5.51$, one-way ANOVA method, followed by Bonferroni post hoc test for multiple comparisons) demonstrated that PF-475 partially reduced total α-synuclein levels in colonic tissues compared to MPTP animals.

LRRK2 antagonist, PF-475, modulated ENS in MPTP-injected mouse colon

During PD pathogenesis, the reduction of ENS proteins present in the colon have often been associated with constipation phenomena and intestinal permeability alterations. To explore the pathophysiology of the ENS in PD, the MPTP animal model is the most studied as this neurotoxin induces neuronal dysfunction and impairment of the ENS as occurs in PD patients.[37] Among these ENS proteins, neuron specific enolase (NSE) and PGP9.5 represent the main markers studied.[38] Expression levels of PGP9.5 and NSE were significantly reduced in PD mice compared to control mice (Figures 6A and 6B, see densitometric analysis A1 and B1, respectively). In contrast, intraperitoneal treatment with PF-475 at the doses of 5 mg/kg and 10 mg/kg considerably increased the expression of PGP9.5 compared to MPTP mouse (Figure 6A, see densitometric

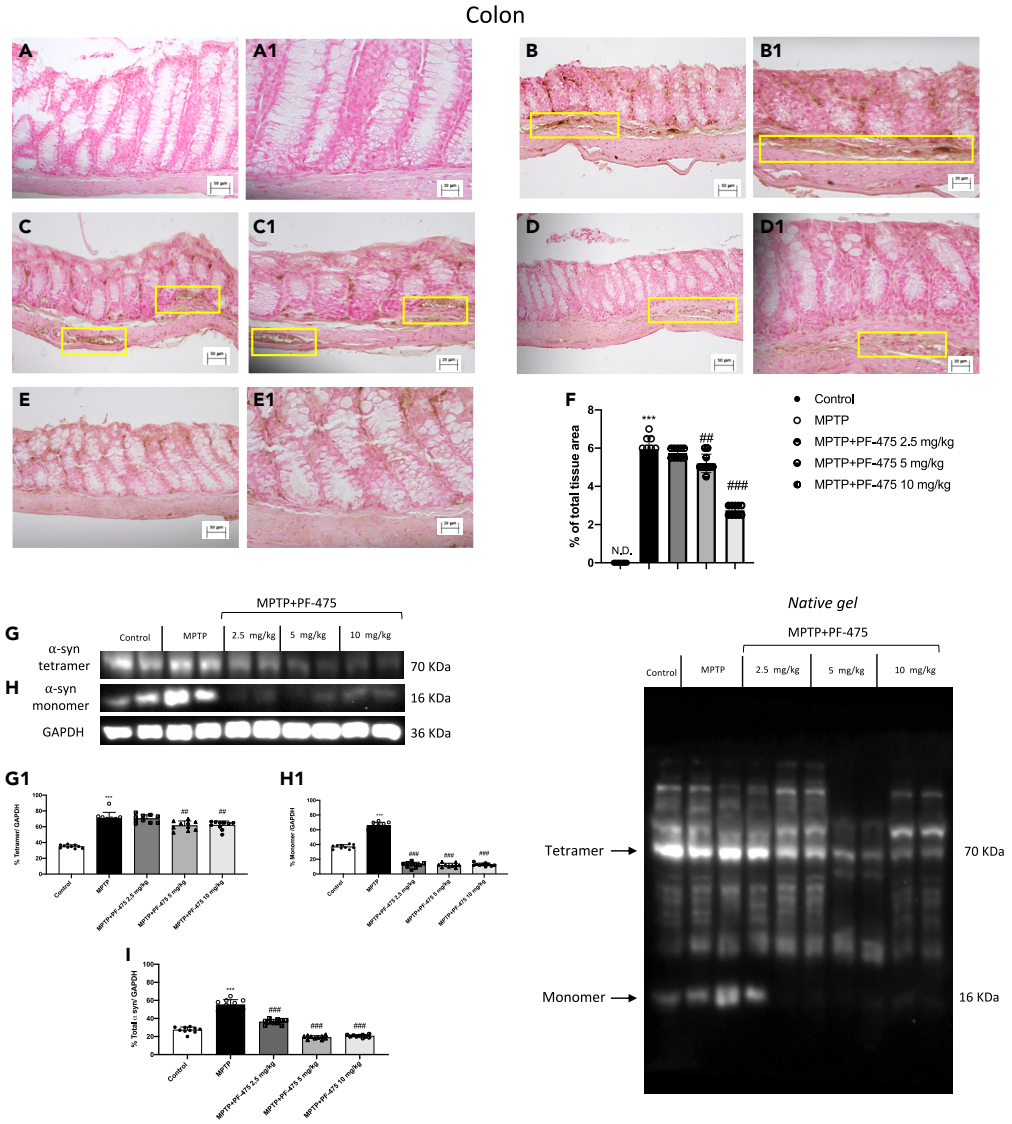

Figure 5. PF-475 treatment preserved α-syn accumulation in colon tissue

Immunohistochemical localization of α-syn after MPTP in colon tissue. Control group (A, A1; see score F), MPTP group (B, B1; see score F), PF-475 2.5 mg/kg treatments after MPTP (C, C1; see score F), PF-475 5 mg/kg treatments after MPTP (D, D1; see score F) and PF-475 10 mg/kg treatments after MPTP (E, E1; see score F; $p = 0.4$; $F(4,45) = 2.84$, one-way ANOVA method, followed by Bonferroni post hoc test for multiple comparisons). Representative western blot of α-syn tetramer and monomer protein expression level in colon tissues after MPTP intoxication and PF-475 treatments (G and H; see densitometric analysis G1, H1, respectively; $p = 0.001$; $F(4,45) = 1.25$, one-way ANOVA method, followed by Bonferroni post hoc test for multiple comparisons; $p = 0.001$; $F(4,45) = 2.81$, respectively for G1 and H1). Representative Western blot of total α-syn protein expression level in colon tissues after MPTP intoxication and PF-475 treatments (densitometric analysis I; $p = 0.001$; $F(4,45) = 5.51$, one-way ANOVA method, followed by Bonferroni post hoc test for multiple comparisons). Data are representative of at least three independent experiments. Values are means ± SD. Distribution of values come from individual animals. One-way ANOVA test. ***$p < 0.001$ vs. control; ##$p < 0.01$ vs. MPTP; ###$p < 0.001$ vs. MPTP.

analysis A1; $p = 0.98$; $F(4,45) = 0.110$, one-way ANOVA method, followed by Bonferroni post hoc test for multiple comparisons). Whereas intraperitoneal treatment with PF-475 at the highest dose of 10 mg/kg increased enteric neuronal marker NSE compared to MPTP mouse (Figure 6B, see densitometric analysis B1; $p = 0.36$; $F(4,45) = 1.12$, one-way ANOVA method, followed by Bonferroni post hoc test for multiple comparisons). It has been shown that the accumulation of α-syn may be accompanied by a loss of neuropeptides such as NSE.[39,40] Therefore, although further studies are needed, this partial increase in NSE following treatment with PF-475 (10 mg/kg) could be related to its protective effect on reducing α-syn accumulation in the colon. In addition, the distribution of neural population of PGP9.5 proteins was observed in immunohistochemistry analysis to confirm whether the western blot results were well reflected. Interestingly, PGP9.5-positive neuronal cells were strongly reduced in colonic sections of MPTP-injected mice (Figure 6D, objective lens 20× D1, see score H) compared with colonic sections of control

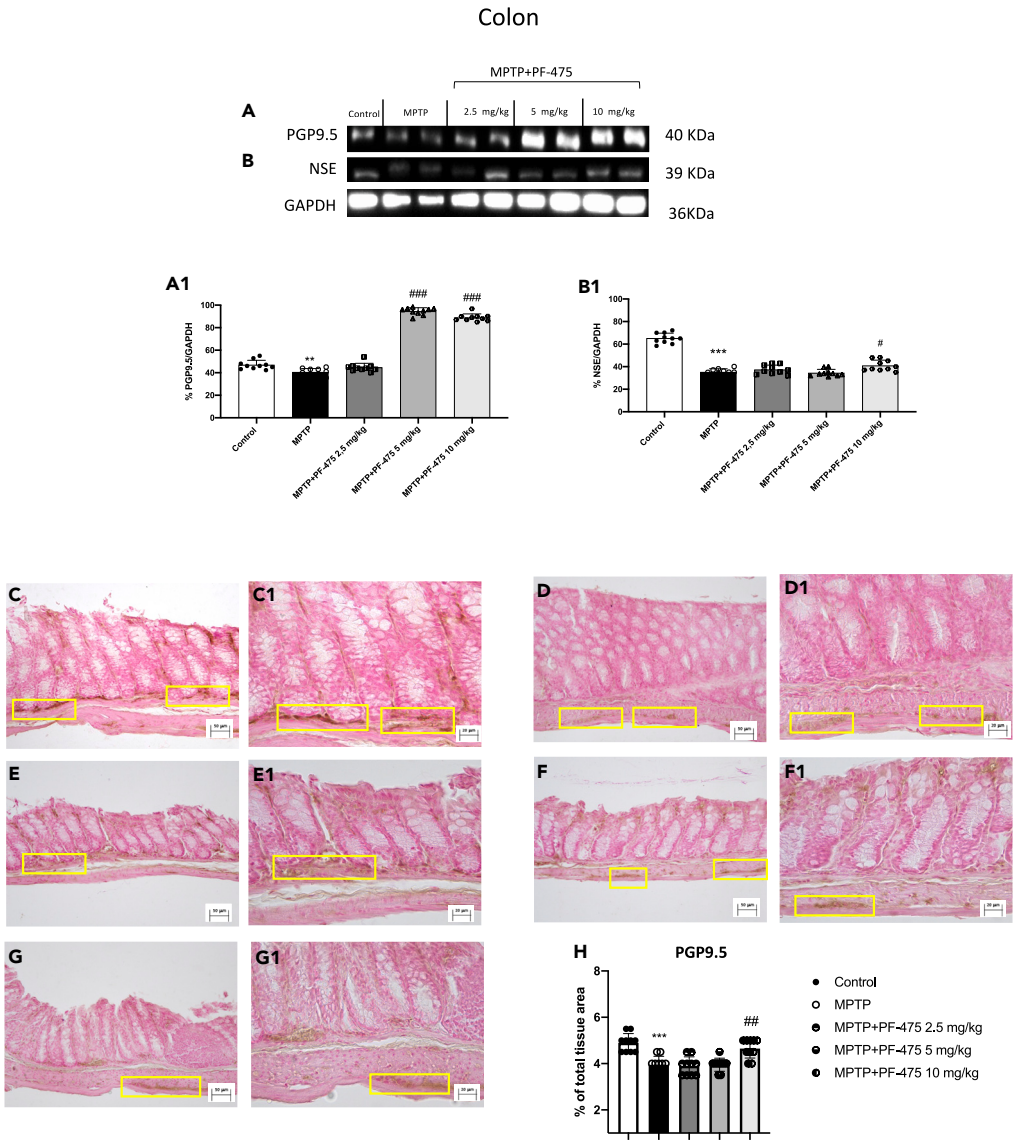

Figure 6. Effect of PF-475 on ENS in MPTP-injected mouse colon

Representative western blot of ENS proteins such as PGP9.5 and NSE in cytosolic fraction of colon tissues after MPTP and PF-475 treatments (A; $p = 0.98$; F (4,45) = 0.110, one-way ANOVA method, followed by Bonferroni post hoc test for multiple comparisons) (B; $p = 0.36$; F (4,45) = 1.12, one-way ANOVA method, followed by Bonferroni post hoc test for multiple comparisons), see densitometric analysis (A1, B1, respectively). Immunohistochemical localization of PGP9.5 after MPTP intoxication in colon tissue. Control group (C, C1; see score H), MPTP group (D, D1; see score H), PF-475 2.5 mg/kg treatments after MPTP (E, E1; see score H), PF-475 5 mg/kg treatments after MPTP (F, F1; see score H; $p = 0.45$; F (4,45) = 0.941, one-way ANOVA method, followed by Bonferroni post hoc test for multiple comparisons) and PF-475 10 mg/kg treatments after MPTP (G, G1; see score F). Data are representative of at least three independent experiments. Values are means ± SD. Distribution of values come from individual animals. One-way ANOVA test. ** <0.01 vs. control; ***$p < 0.001$ vs. control; #$p < 0.05$ vs. MPTP; ##$p < 0.01$ vs. MPTP; ###$p < 0.001$ vs. MPTP.

mice (Figure 6C, objective lens 20× C1, see score H). Selective inhibition of LRRK2 significantly reduced the loss of PGP 9.5 positive cells showing in colonic sections of mice treated with PF-475, at the higher dose of 10 mg/kg an increase in PGP 9.5 positive cells in the submucosal layer and the muscle layer (Figure 6G, objective lens 20× G1, see score H; $p = 0.45$; F (4,45) = 0.941, one-way ANOVA method, followed by Bonferroni post hoc test for multiple comparisons) compared to MPTP-injected mice. These results provide a basis for unveiling that selective LRRK2 inhibition in the colon also modulates enteric nervous system markers during synucleinopathies.

PF-475 reduced colon inflammation through mitophagy pathway

The dysfunction of autophagic pathways characteristic of neurodegeneration in PD is also strongly implicated in inflammatory bowel disease (IBD), leading to impaired intestinal epithelial barrier function, disrupted microbiome, and defective antibacterial peptide secretion.

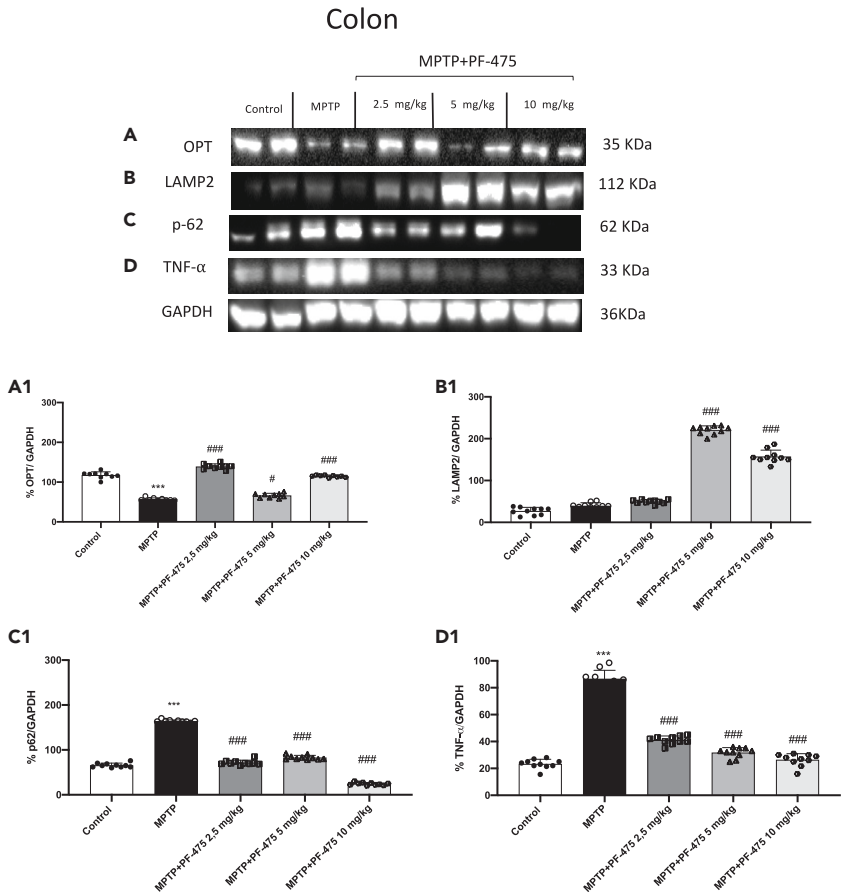

Figure 7. Effect of PF-475 on mitophagy pathway in MPTP-injected mouse colon

Cytosolic fractions of colon tissues were used to evaluate mitophagic protein expression such as OPT, LAMP2 and p62 and pro-inflammatory cytokine TNF-α after MPTP intoxication and PF-475 treatments. Representative western blot of mitophagic protein are shown (A–C), see densitometric analysis of OPT (A1; $p = 0.28$; F (4,45) = 1.33, one-way ANOVA method, followed by Bonferroni post hoc test for multiple comparisons) LAMP2 (B1; $p = 0.31$; F (4,45) = 1,23, one-way ANOVA method, followed by Bonferroni post hoc test for multiple comparisons) and p62 (C1; $p = 0.79$; F (4,45) = 0.420, one-way ANOVA method, followed by Bonferroni post hoc test for multiple comparisons). Expression levels of pro-inflammatory cytokine TNF-α are shown (D, see densitometric analysis D1; $p = 0.44$; F (4,45) = 0.957, one-way ANOVA method, followed by Bonferroni post hoc test for multiple comparisons). Data are representative of at least three independent experiments. Values are means ± SD. Distribution of values come from individual animals. One-way ANOVA test. ***$p < 0.001$ vs. control; #$p < 0.05$ vs. MPTP; ###$p < 0.001$ vs. MPTP.

Furthermore, substantial evidence indicates that LRRK2 mutations play a key role in the autophagy/lysosomal pathway linking PD to colon dysfunction.[41–44] Therefore, once we demonstrated that PF-475 could modulate mitophagy proteins in brain tissue, we aimed to investigate the effect of LRRK2 inhibition on mitophagy marker in the colon of mouse with PD. Consistent with the data obtained in brain tissues, MPTP induced an alteration of autophagic processes also in the colon. Particularly, western blot analysis was performed to investigate the selective mitophagy receptors such as OPT, p62, and LAMP2 involved in the recognition of the ubiquitinated cargo to connect it to the autophagosome membrane. Our results demonstrated a significant reduction of OPT (Figure 7A, see densitometric analysis A1; $p = 0.28$; F (4,45) = 1.33, one-way ANOVA method, followed by Bonferroni post hoc test for multiple comparisons) and an increase of p62 (Figure 7C, see densitometric analysis C1, $p = 0.79$; F (4,45) = 0.420, one-way ANOVA method, followed by Bonferroni post hoc test for multiple comparisons) in colon tissues of MPTP mice compared to control animals. However, PF-475 treatment improved mitophagy by increasing OPT expression and reducing p62. Particularly, PF-475 at all administered doses significantly increased OPT expression levels compared to MPTP-injected mice. In contrast, PF-475 treatment, at all doses, reduced p62 compared to MPTP mice. Moreover, the higher doses of PF-475 (5 mg/kg and 10 mg/kg) were able to significantly increase LAMP2 levels compared to MPTP mice. Furthermore, we also wanted to evaluate TNF-α which is a major pro-inflammatory cytokine that accelerates intestinal damage. As shown in Figure 7D, the levels of this cytokine were significantly increased after administration of MPTP compared to control mice. Consistently, the increase in production of this cytokine in colonic tissues was suppressed in a dose-dependent manner following the administration with PF-475 at a dose of 2.5 mg/kg, 5 mg/kg, and 10 mg/kg compared to MPTP-injected mice (Figure 7D, see densitometric analysis D1; $p = 0.44$; F (4,45) = 0.957, one-way ANOVA method, followed by Bonferroni post hoc test for multiple comparisons). Moreover, to evaluate mitochondrial function we measured ATP and lipid peroxidation

levels by MDA assay, in colon tissues.[45] Our results showed that the colon of MPTP mice exhibited mitochondrial dysfunction revealed by increased MDA levels and decreased ATP levels compared to control mice (Figures S4C and S4D). However, improved mitochondrial function was observed following treatment with PF-475 at dose of 10 mg/kg as indicated by a significant increase in ATP levels and a decrease in MDA production, in colon tissues. Taken together, our data confirmed that the resolution of MPTP-induced intestinal damage could be closely related to autophagy activation mediated by LRRK2 inhibition.

PF-475 reverse alterations in intestinal barrier function in colon of MPTP mice

Since several studies demonstrated that PD patients had high intestinal permeability related to the disorganization of tight junction (TJ) proteins,[46,47] we investigated, by immunofluorescence analysis, the effects of PF-475 on the modulation of zonula occluden-1 (ZO-1) and occludin that are pivotal proteins that regulate the paracellular permeability in intestinal epithelial cells. In this study, we demonstrated that, in colon tissue, MPTP induced a significant decrease in the number of ZO-1 (Figure 8B, see score F) and occludin-positive cells (Figure 8H, see score L) compared to control animals (Figure 8A and G, see score F and L). However, PF-475 treatments at the doses of 5 mg/kg and 10 mg/kg increased the number of occludin (Figures 8D and 8E, see score F, $p = 0.89$; $F(4,45) = 0.277$, one-way ANOVA method, followed by Bonferroni post hoc test for multiple comparisons) and ZO-1 positive cells (Figures 8J and 8K, see score L, $p = 0.85$; $F(4,45) = 0.341$, one-way ANOVA method, followed by Bonferroni post hoc test for multiple comparisons) compared to MPTP-injected mice. To confirm that selective inhibition of LRRK2 could protect against the intestinal barrier effects of MPTP we performed western blot analysis of ZO-1 and occludin in colon protein lysate (Figures S2B and S2C, see densitometric analysis B1 and C1, respectively). Data demonstrated reduced levels of ZO-1 and occludin in MPTP mice compared to control mice. PF-475 treatment significantly increased levels of both TJs compared to MPTP mice, confirming a protective role of the intestinal barrier. Furthermore, intraperitoneal injection of the neurotoxin MPTP caused delayed transit and constipation, as demonstrated by daily stool weight analysis (Figure 8M). After five days of treatment with PF-475 stool weight was not significantly affected. In contrast, after six and seven days of treatment with PF-475 at the doses of 5 mg/kg and 10 mg/kg the stool weight was significantly increased, compared with the MPTP-injected mice. Thus, PF-47 significantly reduced the alteration of gut permeability in MPTP mouse, reducing the loss of TJ proteins.

DISCUSSION

Since LRRK2 is a kinase widely and ubiquitously expressed in immune cells, blood cells, gut lumen, and neuronal cells, it has been thought to be one of the predictive risk factors for PD, IBD, Crohn's disease (CD), and also tumors.[4,48,49] We confirmed increased LRRK2 expression in the brains of MPTP mice, which is consistent with the elevated expression of LRRK2[31] in the colon of MPTP mice. Indeed, LRRK2 contributed to the colon impairments while LRRK2 downregulation by using PF-06447475 inhibitor displayed less serious gastrointestinal consequences after MPTP injection than control mice successfully suggesting an improvement of gastrointestinal system functionality. Although the primary mechanism of PD pathogenesis is still unclear, mitochondrial dysfunction has been increasingly confirmed to be a dynamic contributor. That is because neurotoxins injection to reproduce PD models, including MPTP, damages mitochondrial function by inhibiting its complex core activity and causing the activation of mitophagy to degrade organelles and misfolded proteins. Our observations go further with the alterations in CNS postulating that PD originates in the gastrointestinal tract and that the appearance of α-synuclein accumulation initially occurs, in the earliest stage of PD, in the ENS. Indeed, LRRK2 inhibition in colon of PD mice protected gastrointestinal system from intestinal inflammation mediated by NF-κB that was interestingly enhanced by MPTP and that was inversely decreased from LRRK2 inhibition, indicating that LRRK2 down regulation is controlled in NF-κB-dependent manner. Moreover, through mitophagy, altered intestinal cells regulate both the number and quality of mitochondria in response to the toxic stress from MPTP injection.[50] Our study shows that the damaged colonocytes in the colonic tissue are susceptible from MPTP and that results in a modulation of mitophagy driven by OPT, LAMP-2, and p62 present in enteric neuronal mitochondria and TNF-a interacts with mitophagy by mediating its functionality. As such, OPT is frequently increased not only in the protein inclusions of PD neurons mainly because defective mitophagy, leading to neurodegeneration but also in gastrointestinal system implicating a role in intestinal homeostasis and disease.[51] Therefore, inhibition of LRRK2 has a direct role in inflammation and in mitophagy functions by positively regulate mitochondrial dynamics and autophagosome-lysosome fusion. Here, this was accompanied by an increase in autophagic flux and higher expression of mitophagy markers in mice treated with LRRK2 inhibitor. Furthermore, it was demonstrated that optineurin and p62 were both involved in PINK1/parkin-dependent sequestrosome-like receptor (SLR) mitophagy and PINK1/Parkin-independent SLR mitophagy. In SLR-dependent mitophagy, activation of the PTEN (or other E3 ligases)-inducible kinase 1 (PINK1)/Parkin pathway leads to ubiquitination of mitochondrial OMM proteins. These then bind cytosolic SLRs and activate the autophagy mechanism. In contrast, in SLR-independent mitophagy, mitochondrial receptor proteins are upregulated on the OMM to allow them to interact with related proteins on the phagophore triggering degradation process.[52] In this context, although it is still unclear how LRRK2 modulates mitophagy, it has recently been demonstrated that the effect of LRRK2 on mitophagy is independent of the PINK1/Parkin pathway.[53] To date, little is known about the role of PGP9.5 in PD. However, high levels of ubiquitin C-terminal hydrolase L1 (UCH-L1) expression were found in LBs throughout the central and peripheral nervous systems at all stages of PD. PGP9.5 belongs to the ubiquitin COOH-terminal hydrolase family and its alteration triggers the stability of the ubiquitin dependent proteolytic system.[38,54] It has been demonstrated that dysregulation of PGP9.5 has been implicated in the accumulation of protein aggregates, including α-syn, during PD.[55] Furthermore, research suggests that in the ENS, alterations in PGP9.5 expression and activity may lead to dysregulation of protein homeostasis and neuronal dysfunction, contributing to the gastrointestinal symptoms associated with PD.[7,56] Although further studies are needed to fully elucidate the role of PGP9.5 in ENS and its contribution to PD, in our data, we found that the expression of PGP9.5 was reduced by MPTP exposure, and this is accompanied by changes in the density of NSE in colonic tissue. In colonic tissue, LRRK2 inhibition leads to a significant decrease in

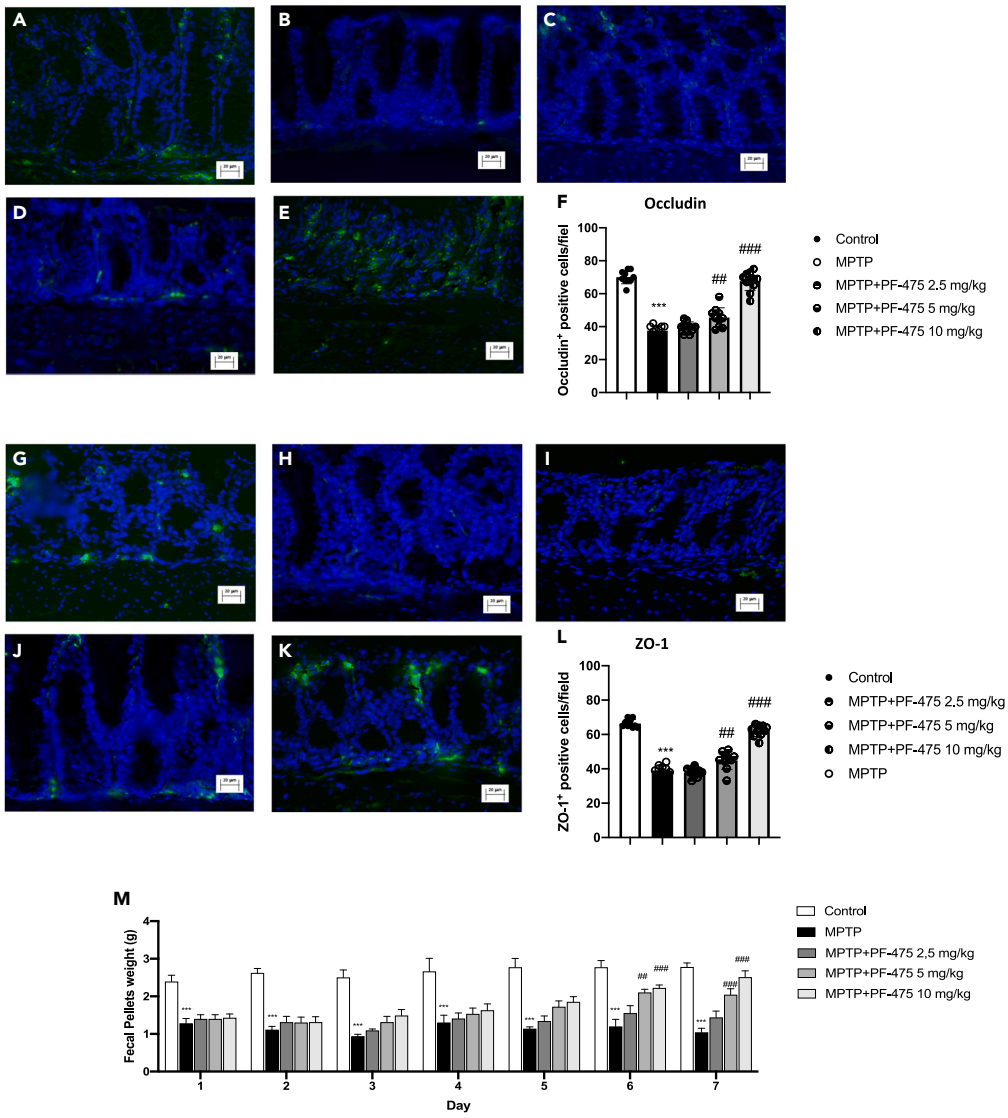

Figure 8. Immunofluorescence analysis of occludin and ZO-1

Colon sections were stained with antibodies against occludin (green) or ZO-1 (green) and DAPI to highlight cell nuclei (blue). Occludin + cells in control group (A, A1); see mean of intensity fluorescence (F). No Occludin + cells were showed in mice subjected to MPTP (B, B1); see mean of intensity fluorescence (F). Mice treated with PF-475 at doses of 2.5 mg/kg (C, C1) see mean of intensity fluorescence (F), and 5 mg/kg (D, D1); see mean of intensity fluorescence (F) and 10 mg/kg (E, E1); see mean of intensity fluorescence (F; $p = 0.89$; F (4,45) = 0.277, one-way ANOVA method, followed by Bonferroni post hoc test for multiple comparisons). ZO-1 + cells in control group (G, G1); see mean of intensity fluorescence (L). No ZO-1+ cells were showed in mice subjected to MPTP (H, H1); see mean of intensity fluorescence (L). Mice treated with PF-475 at doses of 2.5 mg/kg (I, I1) see mean of intensity fluorescence (L), and 5 mg/kg (J, J1); see mean of intensity fluorescence (L) and 10 mg/kg (K, K1); see mean of intensity fluorescence (L; $p = 0.85$; F (4,45) = 0.341, one-way ANOVA method, followed by Bonferroni post hoc test for multiple comparisons). Constipation-related indicator was assessed through determination of fecal weight (M). Data are representative of at least three independent experiments. Values are means ± SD. Distribution of values come from individual animals. One-way ANOVA test. ***$p < 0.001$ vs. control; ##$p < 0.01$ vs. MPTP; ###$p < 0.001$ vs. MPTP.

PGP9.5 and NSE expression along with the restoration of PD-related colon dysfunctions by showing them as a strong predictor of PD outcome. Consistently with studies about LRRK2 inhibitors and LRRK2 $^{-/-}$ mice[4,57] effectively we found ameliorations in colon dysfunction of MPTP mice by using PF-475, and that is because of its exerting action to modulate mitophagy also in colon tissue. We found an abnormal mitochondrial dynamic in the colon of MPTP-mice, a process that basically influences mitochondrial function and autophagy all implicated also in IBD.[58] In the present study, MPTP induction significantly activated mitophagy markers including LAMP2, OPT, p62, and TNF-α expression levels in colon tissues. Also, markers to monitor mitophagy were decreased by LRRK2 inhibition by acting as an upstream coordinator of the degradative process. As changes in mitophagy have been found in the colon of PD mice and after LRRK2 inhibition, dysfunctions of colon

epithelial cells are often accompanied by impairments of barrier integrity and function. In addition, alteration of mitochondrial homeostasis is accompanied by a decrease in mitochondrial oxygen consumption and a reduction in cellular ATP, conditions known to reduce TJs integrity.[59] In this perspective, the evaluation of TJs represented by occludin, and ZO-1 allowed us to confirm that PD triggers in alterations of colon integrity and to discover the contribution of LRRK2 in rebalancing colon barrier alteration from consequent damage. Moreover, constipation is one of the most common gastrointestinal features of PD, and our results demonstrated that PF-475 improved this symptomatology by increasing stool weight. Given the multiple cellular mechanisms of LRRK2 that are dysfunctional in SNpc, and in the colon of PD mice, enhancing mitophagy and improving tissue restoration may rescue PD progression and related diseases. Although it is necessary to confirm the results obtained with a genetic model such as the knockout, in this study we provided several lines of evidence that treatment with the LRRK2 inhibitor improves the barrier and integrity of the colon and attenuates disease-related colon damage of PD.

Limitations of the study

Although this study revealed encouraging results, there are still a few limitations that need to be resolved. First, human diseases are not always possible to translate in preclinical models. Differences in neurodegeneration processes in the context of PD and the correlation of gastrointestinal disorders between mice and humans should be taken into a deep consideration. Moreover, the application of more sophisticated methods will enable a better validation of these preliminary finding, thus providing a more robust characterization of the efficacy of PF-475 in PD-related gastrointestinal disorders. Therefore, future studies using *in vitro* gene silencing models or *in vivo* knockout models will be able to establish in detail the role of LRRK2 in the context of PD-related intestinal disorders.

RESOURCE AVAILABILITY

Lead contact

Further information and requests for resources and reagents should be directed to and will be fulfilled by the Lead Contact, Alessia Filippone (afilippone@unime.it).

Materials availability

This study did not generate new unique reagents.

Data and code availability

- All data reported in this paper will be shared by the lead contact upon request.
- This paper does not report original codes.
- Any additional information required to reanalyze the data reported in this paper is available from the lead contact upon request.

ACKNOWLEDGMENTS

This research was not supported by external fundings.

This study protocol was reviewed and approved by Italian regulations on the use of animals (D.M.116192) and Directive legislation (EU) (2010/63/EU) amended by Regulation (EU) 2019/1010. The animal protocol was approved by Italian Committee (n° 877/2023-PR released on 2023).

AUTHOR CONTRIBUTIONS

All authors contributed equally to the study. Conceptualization and design were performed by A.F. and E.E. Material preparation, data collection and analysis were performed by L.C., F.C., L.C., and I.P. The first draft of the manuscript was written by A.F. and D.M. All authors read and approved the final manuscript.

DECLARATION OF INTERESTS

The authors declare no competing interests.

STAR★METHODS

Detailed methods are provided in the online version of this paper and include the following:

SUPPLEMENTAL INFORMATION

Supplemental information can be found online at https://doi.org/10.1016/j.isci.2024.110980.

Received: January 31, 2024
Revised: May 10, 2024
Accepted: September 13, 2024
Published: September 16, 2024

REFERENCES

1. Shults, C.W. (2006). Lewy bodies. Proc. Natl. Acad. Sci. USA *103*, 1661–1668. https://doi.org/10.1073/pnas.0509567103.
2. Fasano, A., Visanji, N.P., Liu, L.W.C., Lang, A.E., and Pfeiffer, R.F. (2015). Gastrointestinal dysfunction in Parkinson's disease. Lancet Neurol. *14*, 625–639. https://doi.org/10.1016/S1474-4422(15)00007-1.
3. Bu, J., Liu, J., Liu, K., and Wang, Z. (2019). Diagnostic utility of gut alpha-synuclein in Parkinson's disease: A systematic review and meta-analysis. Behav. Brain Res. *364*, 340–347. https://doi.org/10.1016/j.bbr.2019.02.039.
4. Yan, J., Yu, W., Wang, G., Lu, C., Liu, C., Jiang, L., Jiang, Z., Liang, Z., and Liu, D. (2022). LRRK2 deficiency mitigates colitis progression by favoring resolution of inflammation and restoring homeostasis of gut microbiota. Genomics *114*, 110527. https://doi.org/10.1016/j.ygeno.2022.110527.
5. Price, A., Manzoni, C., Cookson, M.R., and Lewis, P.A. (2018). The LRRK2 signalling system. Cell Tissue Res. *373*, 39–50. https://doi.org/10.1007/s00441-017-2759-9.
6. Gilsbach, B.K., Messias, A.C., Ito, G., Sattler, M., Alessi, D.R., Wittinghofer, A., and Kortholt, A. (2015). Structural Characterization of LRRK2 Inhibitors. J. Med. Chem. *58*, 3751–3756. https://doi.org/10.1021/jm5018779.
7. Kurihara, L.J., Kikuchi, T., Wada, K., and Tilghman, S.M. (2001). Loss of Uch-L1 and Uch-L3 leads to neurodegeneration, posterior paralysis and dysphagia. Hum. Mol. Genet. *10*, 1963–1970. https://doi.org/10.1093/hmg/10.18.1963.
8. Filippone, A., Cucinotta, L., Bova, V., Lanza, M., Casili, G., Paterniti, I., Campolo, M., Cuzzocrea, S., and Esposito, E. (2023). Inhibition of LRRK2 Attenuates Depression-Related Symptoms in Mice with Moderate Traumatic Brain Injury. Cells *12*, 1040. https://doi.org/10.3390/cells12071040.
9. Uppala, S.N., Tryphena, K.P., Naren, P., Srivastava, S., Singh, S.B., and Khatri, D.K. (2023). Involvement of miRNA on epigenetics landscape of Parkinson's disease: From pathogenesis to therapeutics. Mech. Ageing Dev. *213*, 111826. https://doi.org/10.1016/j.mad.2023.111826.
10. Chu, C.T. (2010). A pivotal role for PINK1 and autophagy in mitochondrial quality control: implications for Parkinson disease. Hum. Mol. Genet. *19*, R28–R37. https://doi.org/10.1093/hmg/ddq143.
11. Tryphena, K.P., Nikhil, U.S., Pinjala, P., Srivastava, S., Singh, S.B., and Khatri, D.K. (2023). Mitochondrial Complex I as a Pathologic and Therapeutic Target for Parkinson's Disease. ACS Chem. Neurosci. *14*, 1356–1368. https://doi.org/10.1021/acschemneuro.2c00819.
12. Naren, P., Samim, K.S., Tryphena, K.P., Vora, L.K., Srivastava, S., Singh, S.B., and Khatri, D.K. (2023). Microtubule acetylation dyshomeostasis in Parkinson's disease. Transl. Neurodegener. *12*, 20. https://doi.org/10.1186/s40035-023-00354-0.
13. Johansen, T., and Lamark, T. (2011). Selective autophagy mediated by autophagic adapter proteins. Autophagy *7*, 279–296. https://doi.org/10.4161/auto.7.3.14487.
14. Filippone, A., Mannino, D., Cucinotta, L., Paterniti, I., Esposito, E., and Campolo, M. (2022). LRRK2 Inhibition by PF06447475 Antagonist Modulates Early Neuronal Damage after Spinal Cord Trauma. Antioxidants *11*, 1634. https://doi.org/10.3390/antiox11091634.
15. Quintero-Espinosa, D.A., Ortega-Arellano, H.F., Velez-Pardo, C., and Jimenez-Del-Rio, M. (2022). Phenolic-rich extract of avocado Persea americana (var. Colinred) peel blunts paraquat/maneb-induced apoptosis through blocking phosphorylation of LRRK2 kinase in human nerve-like cells. Environ. Toxicol. *37*, 660–676. https://doi.org/10.1002/tox.23433.
16. Nguyen, M., Wong, Y.C., Ysselstein, D., Severino, A., and Krainc, D. (2019). Synaptic, Mitochondrial, and Lysosomal Dysfunction in Parkinson's Disease. Trends Neurosci. *42*, 140–149. https://doi.org/10.1016/j.tins.2018.11.001.
17. Tolosa, E., Vila, M., Klein, C., and Rascol, O. (2020). LRRK2 in Parkinson disease: challenges of clinical trials. Nat. Rev. Neurol. *16*, 97–107. https://doi.org/10.1038/s41582-019-0301-2.
18. Singh, F., and Ganley, I.G. (2021). Parkinson's disease and mitophagy: an emerging role for LRRK2. Biochem. Soc. Trans. *49*, 551–562. https://doi.org/10.1042/BST20190236.
19. Wauters, F., Cornelissen, T., Imberechts, D., Martin, S., Koentjoro, B., Sue, C., Vangheluwe, P., and Vandenberghe, W. (2020). LRRK2 mutations impair depolarization-induced mitophagy through inhibition of mitochondrial accumulation of RAB10. Autophagy *16*, 203–222. https://doi.org/10.1080/15548627.2019.1603548.
20. Khot, M., Sood, A., Tryphena, K.P., Pinjala, P., Srivastava, S., Singh, S.B., and Khatri, D.K. (2023). Dimethyl fumarate ameliorates parkinsonian pathology by modulating autophagy and apoptosis via Nrf2-TIGAR-LAMP2/Cathepsin D axis. Brain Res. *1815*, 148462. https://doi.org/10.1016/j.brainres.2023.148462.
21. Wu, F., Xu, H.D., Guan, J.J., Hou, Y.S., Gu, J.H., Zhen, X.C., and Qin, Z.H. (2015). Rotenone impairs autophagic flux and lysosomal functions in Parkinson's disease. Neuroscience *284*, 900–911. https://doi.org/10.1016/j.neuroscience.2014.11.004.
22. Jin, M.M., Wang, F., Qi, D., Liu, W.W., Gu, C., Mao, C.J., Yang, Y.P., Zhao, Z., Hu, L.F., and Liu, C.F. (2018). A Critical Role of Autophagy in Regulating Microglia Polarization in Neurodegeneration. Front. Aging Neurosci. *10*, 378. https://doi.org/10.3389/fnagi.2018.00378.
23. Yu, S.H., Palanisamy, K., Sun, K.T., Li, X., Wang, Y.M., Lin, F.Y., Chen, K.B., Wang, I.K., Yu, T.M., and Li, C.Y. (2021). Human antigen R regulates hypoxia-induced mitophagy in renal tubular cells through PARKIN/BNIP3L expressions. J. Cell Mol. Med. *25*, 2691–2702. https://doi.org/10.1111/jcmm.16301.
24. Yelamanchili, S.V., Chaudhuri, A.D., Flynn, C.T., and Fox, H.S. (2011). Upregulation of cathepsin D in the caudate nucleus of primates with experimental parkinsonism. Mol. Neurodegener. *6*, 52. https://doi.org/10.1186/1750-1326-6-52.
25. Zhao, N., Yan, Q.W., Xia, J., Zhang, X.L., Li, B.X., Yin, L.Y., and Xu, B. (2020). Treadmill Exercise Attenuates Abeta-Induced Mitochondrial Dysfunction and Enhances Mitophagy Activity in APP/PS1 Transgenic Mice. Neurochem. Res. *45*, 1202–1214. https://doi.org/10.1007/s11064-020-03003-4.
26. Abrahams, S., Miller, H.C., Lombard, C., van der Westhuizen, F.H., and Bardien, S. (2021). Curcumin pre-treatment may protect against mitochondrial damage in LRRK2-mutant Parkinson's disease and healthy control fibroblasts. Biochem. Biophys. Rep. *27*, 101035. https://doi.org/10.1016/j.bbrep.2021.101035.
27. Liu, H.F., Ho, P.W.L., Leung, G.C.T., Lam, C.S.C., Pang, S.Y.Y., Li, L., Kung, M.H.W., Ramsden, D.B., and Ho, S.L. (2017). Combined LRRK2 mutation, aging and chronic low dose oral rotenone as a model of Parkinson's disease. Sci. Rep. *7*, 40887. https://doi.org/10.1038/srep40887.
28. Chen, C., Yang, C., Wang, J., Huang, X., Yu, H., Li, S., Li, S., Zhang, Z., Liu, J., Yang, X., and Liu, G.P. (2021). Melatonin ameliorates cognitive deficits through improving mitophagy in a mouse model of Alzheimer's disease. J. Pineal Res. *71*, e12774. https://doi.org/10.1111/jpi.12774.
29. Manczak, M., Kandimalla, R., Fry, D., Sesaki, H., and Reddy, P.H. (2016). Protective effects of reduced dynamin-related protein 1 against amyloid beta-induced mitochondrial dysfunction and synaptic damage in

Alzheimer's disease. Hum. Mol. Genet. *25*, 5148–5166. https://doi.org/10.1093/hmg/ddw330.

30. Cote, M., Bourque, M., Poirier, A.A., Aube, B., Morissette, M., Di Paolo, T., and Soulet, D. (2015). GPER1-mediated immunomodulation and neuroprotection in the myenteric plexus of a mouse model of Parkinson's disease. Neurobiol. Dis. *82*, 99–113. https://doi.org/10.1016/j.nbd.2015.05.017.
31. Devos, D., Lebouvier, T., Lardeux, B., Biraud, M., Rouaud, T., Pouclet, H., Coron, E., Bruley des Varannes, S., Naveilhan, P., Nguyen, J.M., et al. (2013). Colonic inflammation in Parkinson's disease. Neurobiol. Dis. *50*, 42–48. https://doi.org/10.1016/j.nbd.2012.09.007.
32. Cote, M., Poirier, A.A., Aube, B., Jobin, C., Lacroix, S., and Soulet, D. (2015). Partial depletion of the proinflammatory monocyte population is neuroprotective in the myenteric plexus but not in the basal ganglia in a MPTP mouse model of Parkinson's disease. Brain Behav. Immun. *46*, 154–167. https://doi.org/10.1016/j.bbi.2015.01.009.
33. Cote, M., Drouin-Ouellet, J., Cicchetti, F., and Soulet, D. (2011). The critical role of the MyD88-dependent pathway in non-CNS MPTP-mediated toxicity. Brain Behav. Immun. *25*, 1143–1152. https://doi.org/10.1016/j.bbi.2011.02.017.
34. Natale, G., Kastsiuchenka, O., Pasquali, L., Ruggieri, S., Paparelli, A., and Fornai, F. (2008). MPTP- but not methamphetamine-induced parkinsonism extends to catecholamine neurons in the gut. Ann. N. Y. Acad. Sci. *1139*, 345–349. https://doi.org/10.1196/annals.1432.015.
35. Su, Y., Liu, N., Zhang, Z., Li, H., Ma, J., Yuan, Y., Shi, M., Liu, J., Zhao, Z., Zhang, Z., and Holscher, C. (2022). Cholecystokinin and glucagon-like peptide-1 analogues regulate intestinal tight junction, inflammation, dopaminergic neurons and alpha-synuclein accumulation in the colon of two Parkinson's disease mouse models. Eur. J. Pharmacol. *926*, 175029. https://doi.org/10.1016/j.ejphar.2022.175029.
36. Seo, M.H., Kwon, D., Kim, S.H., and Yeo, S. (2023). Association between Decreased SGK1 and Increased Intestinal alpha-Synuclein in an MPTP Mouse Model of Parkinson's Disease. Int. J. Mol. Sci. *24*, 16408. https://doi.org/10.3390/ijms242216408.
37. Anderson, G., Noorian, A.R., Taylor, G., Anitha, M., Bernhard, D., Srinivasan, S., and Greene, J.G. (2007). Loss of enteric dopaminergic neurons and associated changes in colon motility in an MPTP mouse model of Parkinson's disease. Exp. Neurol. *207*, 4–12. https://doi.org/10.1016/j.expneurol.2007.05.010.
38. Choi, Y.J., Song, H.J., Kim, J.E., Lee, S.J., Jin, Y.J., Roh, Y.J., Seol, A., Kim, H.S., and Hwang, D.Y. (2022). Dysregulation of the Enteric Nervous System in the Mid Colon of Complement Component 3 Knockout Mice with Constipation Phenotypes. Int. J. Mol. Sci. *23*, 6862. https://doi.org/10.3390/ijms23126862.
39. Bottner, M., Zorenkov, D., Hellwig, I., Barrenschee, M., Harde, J., Fricke, T., Deuschl, G., Egberts, J.H., Becker, T., Fritscher-Ravens, A., et al. (2012). Expression pattern and localization of alpha-synuclein in the human enteric nervous system. Neurobiol. Dis. *48*, 474–480. https://doi.org/10.1016/j.nbd.2012.07.018.
40. Kim, J.E., Kwon, K.C., Jin, Y.J., Seol, A., Song, H.J., Roh, Y.J., Kim, T.R., Park, E.S., Park, G.H., Park, J.W., et al. (2023). Compositional changes in fecal microbiota in a new Parkinson's disease model: C57BL/6-Tg(NSE-haSyn) mice. Lab. Anim. Res. *39*, 30. https://doi.org/10.1186/s42826-023-00181-4.
41. Zhang, K., Zhu, S., Li, J., Jiang, T., Feng, L., Pei, J., Wang, G., Ouyang, L., and Liu, B. (2021). Targeting autophagy using small-molecule compounds to improve potential therapy of Parkinson's disease. Acta Pharm. Sin. B *11*, 3015–3034. https://doi.org/10.1016/j.apsb.2021.02.016.
42. Smolders, S., and Van Broeckhoven, C. (2020). Genetic perspective on the synergistic connection between vesicular transport, lysosomal and mitochondrial pathways associated with Parkinson's disease pathogenesis. Acta Neuropathol. Commun. *8*, 63. https://doi.org/10.1186/s40478-020-00935-4.
43. Sosero, Y.L., and Gan-Or, Z. (2023). LRRK2 and Parkinson's disease: from genetics to targeted therapy. Ann. Clin. Transl. Neurol. *10*, 850–864. https://doi.org/10.1002/acn3.51776.
44. Filippone, A., Smith, T., and Pratico, D. (2021). Dysregulation of the Retromer Complex in Brain Endothelial Cells Results in Accumulation of Phosphorylated Tau. J. Inflamm. Res. *14*, 7455–7465. https://doi.org/10.2147/JIR.S342096.
45. Heller, S., Penrose, H.M., Cable, C., Biswas, D., Nakhoul, H., Baddoo, M., Flemington, E., Crawford, S.E., and Savkovic, S.D. (2017). Reduced mitochondrial activity in colonocytes facilitates AMPKalpha2-dependent inflammation. Faseb. J. *31*, 2013–2025. https://doi.org/10.1096/fj.201600976R.
46. Forsyth, C.B., Shannon, K.M., Kordower, J.H., Voigt, R.M., Shaikh, M., Jaglin, J.A., Estes, J.D., Dodiya, H.B., and Keshavarzian, A. (2011). Increased intestinal permeability correlates with sigmoid mucosa alpha-synuclein staining and endotoxin exposure markers in early Parkinson's disease. PLoS One *6*, e28032. https://doi.org/10.1371/journal.pone.0028032.
47. Clairembault, T., Leclair-Visonneau, L., Coron, E., Bourreille, A., Le Dily, S., Vavasseur, F., Heymann, M.F., Neunlist, M., and Derkinderen, P. (2015). Structural alterations of the intestinal epithelial barrier in Parkinson's disease. Acta Neuropathol. Commun. *3*, 12. https://doi.org/10.1186/s40478-015-0196-0.
48. Dickson, D.W., Braak, H., Duda, J.E., Duyckaerts, C., Gasser, T., Halliday, G.M., Hardy, J., Leverenz, J.B., Del Tredici, K., Wszolek, Z.K., and Litvan, I. (2009). Neuropathological assessment of Parkinson's disease: refining the diagnostic criteria. Lancet Neurol. *8*, 1150–1157. https://doi.org/10.1016/S1474-4422(09)70238-8.
49. Jiang, Z.C., Chen, X.J., Zhou, Q., Gong, X.H., Chen, X., and Wu, W.J. (2019). Downregulated LRRK2 gene expression inhibits proliferation and migration while promoting the apoptosis of thyroid cancer cells by inhibiting activation of the JNK signaling pathway. Int. J. Oncol. *55*, 21–34. https://doi.org/10.3892/ijo.2019.4816.
50. Wang, B., Abraham, N., Gao, G., and Yang, Q. (2016). Dysregulation of autophagy and mitochondrial function in Parkinson's disease. Transl. Neurodegener. *5*, 19. https://doi.org/10.1186/s40035-016-0065-1.
51. Wise, J.P., Jr., Price, C.G., Amaro, J.A., and Cannon, J.R. (2018). Autophagy Disruptions Associated With Altered Optineurin Expression in Extranigral Regions in a Rotenone Model of Parkinson's Disease. Front. Neurosci. *12*, 289. https://doi.org/10.3389/fnins.2018.00289.
52. Onishi, M., Yamano, K., Sato, M., Matsuda, N., and Okamoto, K. (2021). Molecular mechanisms and physiological functions of mitophagy. EMBO J. *40*, e104705. https://doi.org/10.15252/embj.2020104705.
53. Singh, F., Prescott, A.R., Rosewell, P., Ball, G., Reith, A.D., and Ganley, I.G. (2021). Pharmacological rescue of impaired mitophagy in Parkinson's disease-related LRRK2 G2019S knock-in mice. Elife *10*, e67604. https://doi.org/10.7554/eLife.67604.
54. Satoh, J.I., and Kuroda, Y. (2001). Ubiquitin C-terminal hydrolase-L1 (PGP9.5) expression in human neural cell lines following induction of neuronal differentiation and exposure to cytokines, neurotrophic factors or heat stress. Neuropathol. Appl. Neurobiol. *27*, 95–104. https://doi.org/10.1046/j.1365-2990.2001.00313.x.
55. Ortega Moreno, L., Bagues, A., Martinez, V., and Abalo, R. (2023). New Pieces for an Old Puzzle: Approaching Parkinson's Disease from Translatable Animal Models, Gut Microbiota Modulation, and Lipidomics. Nutrients *15*, 2775. https://doi.org/10.3390/nu15122775.
56. Coulombe, J., Gamage, P., Gray, M.T., Zhang, M., Tang, M.Y., Woulfe, J., Saffrey, M.J., and Gray, D.A. (2014). Loss of UCHL1 promotes age-related degenerative changes in the enteric nervous system. Front. Aging Neurosci. *6*, 129. https://doi.org/10.3389/fnagi.2014.00129.
57. Takagawa, T., Kitani, A., Fuss, I., Levine, B., Brant, S.R., Peter, I., Tajima, M., Nakamura, S., and Strober, W. (2018). An increase in LRRK2 suppresses autophagy and enhances Dectin-1-induced immunity in a mouse model of colitis. Sci. Transl. Med. *10*, eaan8162. https://doi.org/10.1126/scitranslmed.aan8162.
58. Liang, D., Zhuo, Y., Guo, Z., He, L., Wang, X., He, Y., Li, L., and Dai, H. (2020). SIRT1/PGC-1 pathway activation triggers autophagy/mitophagy and attenuates oxidative damage in intestinal epithelial cells. Biochimie *170*, 10–20. https://doi.org/10.1016/j.biochi.2019.12.001.
59. Dickman, K.G., Hempson, S.J., Anderson, J., Lippe, S., Zhao, L., Burakoff, R., and Shaw, R.D. (2000). Rotavirus alters paracellular permeability and energy metabolism in Caco-2 cells. Am. J. Physiol. Gastrointest. Liver Physiol. *279*, G757–G766. https://doi.org/10.1152/ajpgi.2000.279.4.G757.
60. Campolo, M., Casili, G., Lanza, M., Filippone, A., Paterniti, I., Cuzzocrea, S., and Esposito, E. (2018). Multiple mechanisms of dimethyl fumarate in amyloid beta-induced neurotoxicity in human neuronal cells. J. Cell Mol. Med. *22*, 1081–1094. https://doi.org/10.1111/jcmm.13358.
61. Mendivil-Perez, M., Velez-Pardo, C., and Jimenez-Del-Rio, M. (2016). Neuroprotective Effect of the LRRK2 Kinase Inhibitor PF-06447475 in Human Nerve-Like Differentiated Cells Exposed to Oxidative Stress Stimuli: Implications for Parkinson's Disease. Neurochem. Res. *41*, 2675–2692. https://doi.org/10.1007/s11064-016-1982-1.
62. Natale, G., Kastsiushenka, O., Fulceri, F., Ruggieri, S., Paparelli, A., and Fornai, F. (2010). MPTP-induced parkinsonism extends

to a subclass of TH-positive neurons in the gut. Brain Res. *1355*, 195–206. https://doi.org/10.1016/j.brainres.2010.07.076.

63. Segui-Gomez, M., Plasencia, A., and Borrell, C. (1996). Quality of emergency diagnosis of lesions of external causes requiring hospitalization. Gac. Sanit. *10*, 110–116. https://doi.org/10.1016/s0213-9111(96)71884-8.
64. Ellett, L.J., Hung, L.W., Munckton, R., Sherratt, N.A., Culvenor, J., Grubman, A., Furness, J.B., White, A.R., Finkelstein, D.I., Barnham, K.J., and Lawson, V.A. (2016). Restoration of intestinal function in an MPTP model of Parkinson's Disease. Sci. Rep. *6*, 30269. https://doi.org/10.1038/srep30269.
65. Filippone, A., Casili, G., Ardizzone, A., Lanza, M., Mannino, D., Paterniti, I., Esposito, E., and Campolo, M. (2021). Inhibition of Prolyl Oligopeptidase Prevents Consequences of Reperfusion following Intestinal Ischemia. Biomedicines *9*, 1354. https://doi.org/10.3390/biomedicines9101354.
66. Liberatore, G.T., Jackson-Lewis, V., Vukosavic, S., Mandir, A.S., Vila, M., McAuliffe, W.G., Dawson, V.L., Dawson, T.M., and Przedborski, S. (1999). Inducible nitric oxide synthase stimulates dopaminergic neurodegeneration in the MPTP model of Parkinson disease. Nat. Med. *5*, 1403–1409. https://doi.org/10.1038/70978.
67. Ardizzone, A., Filippone, A., Mannino, D., Scuderi, S.A., Casili, G., Lanza, M., Cucinotta, L., Campolo, M., and Esposito, E. (2022). Ulva pertusa, a Marine Green Alga, Attenuates DNBS-Induced Colitis Damage via NF-kappaB/Nrf2/SIRT1 Signaling Pathways. J. Clin. Med. *11*, 4301. https://doi.org/10.3390/jcm11154301.
68. Ardizzone, A., Mannino, D., Capra, A.P., Repici, A., Filippone, A., Esposito, E., and Campolo, M. (2023). New Insights into the Mechanism of Ulva pertusa on Colitis in Mice: Modulation of the Pain and Immune System. Mar. Drugs *21*, 298. https://doi.org/10.3390/md21050298.
69. Lee, H.Y., Kim, J.H., Jeung, H.W., Lee, C.U., Kim, D.S., Li, B., Lee, G.H., Sung, M.S., Ha, K.C., Back, H.I., et al. (2012). Effects of Ficus carica paste on loperamide-induced constipation in rats. Food Chem. Toxicol. *50*, 895–902. https://doi.org/10.1016/j.fct.2011.12.001.
70. Wang, Y., Chen, W.J., Han, Y.Y., Xu, X., Yang, A.X., Wei, J., Hong, D.J., Fang, X., and Chen, T.T. (2023). Neuroprotective effect of engineered Clostridiumbutyricum-pMTL007-GLP-1 on Parkinson's disease mice models via promoting mitophagy. Bioeng. Transl. Med. *8*, e10505. https://doi.org/10.1002/btm2.10505.
71. Filippone, A., Lanza, M., Campolo, M., Casili, G., Paterniti, I., Cuzzocrea, S., and Esposito, E. (2020). Protective effect of sodium propionate in Abeta(1-42) -induced neurotoxicity and spinal cord trauma. Neuropharmacology *166*, 107977. https://doi.org/10.1016/j.neuropharm.2020.107977.

STAR★METHODS

KEY RESOURCES TABLE

REAGENT or RESOURCE	SOURCE	IDENTIFIER
Antibodies		
Rabbit monoclonal anti-LRRK2	Abcam	ab-133474
Rabbit monoclonal anti-phosphorylated LRRK2	Abcam	ab-133450
Mouse monoclonal anti-iNOS	Santa Cruz Biotechnology	sc-7271
Mouse monoclonal anti-COX2	Santa Cruz Biotechnology	sc-376861
Rabbit polyclonal anti- α-synuclein	Santa Cruz Biotechnology	sc-7011
Rabbit polyclonal anti-PGP9.5	Elabscience	E-AB-53097
Rabbit polyclonal anti-NSE	Invitrogen	PA5-94940
Rabbit polyclonal anti-p62	Abcam	ab91526
Mouse monoclonal anti-LAMP2	Invitrogen	MA1-205
Rabbit monoclonal anti-RAB12(phosphor S106)	Abcam	ab256487
Rabbit polyclonal anti-RAB12	Proteintech	18843-1-AP
Rabbit monoclonal anti-RAB10(phosphor T73)	Abcam	ab230261
Mouse monoclonal anti-RAB10	Abcam	ab104859
Mouse monoclonal anti-Occludin	Santa Cruz Biotechnology	sc-133256
Mouse monoclonal anti-ZO-1	Santa Cruz Biotechnology	sc-33725
Mouse monoclonal anti-β-actin	Santa Cruz Biotechnology	sc-47778
Chemicals, peptides, and recombinant proteins		
PF06447475	MedChemExpress LLC	HY-12477
Precision Plus protein unstained Standards	Bio-Rad	64333538
Critical commercial assays		
Mouse IL-1β ELISA Kit	Abcam	ab197742
Mouse ATP ELISA kit	MyBiosource	MBS267352
Experimental models: Cell lines		
SH-SY5Y	ATCC®	CRL-2266™
Experimental models: Organisms/strains		
Mouse CD1	Envigo/Inotiv	
Software and algorithms		
ImageJ	Fiji	Version 1.53
GraphPad 9.0	Prism	Version 8.4

EXPERIMENTAL MODEL AND STUDY PARTICIPANT DETAILS

Cell cultures

Human neuroblastoma cells (SH-SY5Y cell line) (ATCC® CRL-2266™, derived from the parental SK-N-SH female human neuroblastoma cell line) were seeded 8 × 10^5 cells and plated in 6-wells plate. Then, cells were incubated with retinoic acid (100 nM) for 24 h to induce differentiation into mature neurons.[60] Cells were After this time, cells were pretreated for 2 h with PF-475 (1 and 3 μM) followed by addition of MPTP (3 mM). After 24 h, cell lysates were prepared for western blot analysis as previously described.[60] The concentration of MPTP and PF-475 used was based on previous *in vitro* studies.[61]

Differentiated SH-SY5Y cells were divided into 4 groups:

1. Control cells: differentiated cells were cultured with basal medium;
2. MPTP treated cells: differentiated cells were treated with 3 mM of MPTP;
3. MPTP+PF-475 1 μM treated cells: differentiated cells were treated with 1 μM PF-475 for 2 h before addition of 3 mM of MPTP for 24 h;
4. MPTP+ PF-475 3 μM treated cells: differentiated cells were treated with 3 μM PF-475 for 2 h before addition of 3 mM of MPTP for 24 h.

Animals

CD1 male mice (25–30 g; 6–8 weeks of age) were purchased from Envigo (Milan, Italy). The mice were placed in a controlled environment and were fed with standard rodent food and water *ad libitum*. The animals were housed in stainless steel cages in a room maintained at 22 ± 1°C with a cycle of 12 h of light and 12 h of dark. The animal study was performed in accordance with Italian regulations on the use of animals (D.M.116192) and Directive legislation (EU) (2010/63/EU) amended by Regulation (EU) 2019/1010. The animal protocol was approved by Italian Committee (n° 877/2023-PR released on 2023).

METHOD DETAILS

Materials

PF06447475 (abbreviated as PF-475) was purchased from MedChemExpress LLC (1 Deer Park Dr, Suite Q, Monmouth Junction, NJ 08852, USA; # HY-12477). All stock solutions were prepared in nonpyrogenic saline (0.9% NaCl; Baxter, Liverpool, UK). Unless otherwise stated, all compounds were obtained from Sigma–Aldrich (Milan, Italy).

Induction of MPTP mouse model

Adult male CD1 mice received four intraperitoneal injections of 1-methyl-4-phenyl-1,2,3,6-tetrahydropyridine (MPTP) (20 mg/kg; Sigma-Aldrich, St. Louis, MO) in saline at 2 h intervals in 1 day and the total dose for each mouse was 80 mg/kg. Starting 24 h after the first MPTP injection, animals received intraperitoneal administration of PF-475 at doses of 2.5 mg/kg ,5 mg/kg and 10 mg/kg respectively. PF-475 was administered once daily until 7 days after the MPTP injection. PF-475 was dissolved in dimethyl sulfoxide (DMSO) and diluted with 0.9% saline to a final concentration of <1% DMSO (see the table below).[14] 7 days after MPTP injection brains and colon were collected and used for further analysis (Experimental timeline).

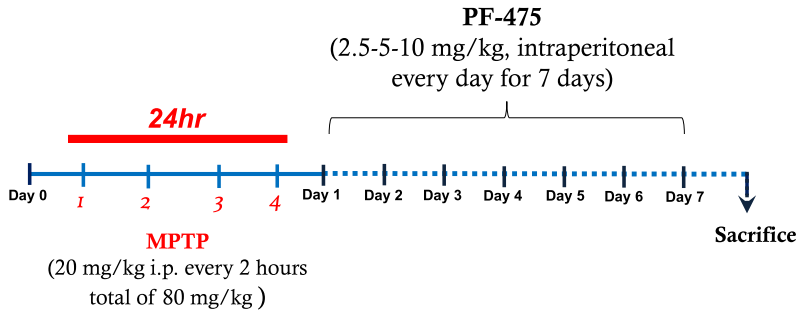

EXPERIMENTAL GROUPS
❖ Control n=10
❖ Contro+PF-475 2.5 mg/kg n=10
❖ Contro+PF-475 5 mg/kg n=10
❖ Contro+PF-475 10 mg/kg n=10
❖ MPTP n=10
❖ MPTP + PF-475 2.5 mg/kg n=10
❖ MPTP + PF-475 5 mg/kg n=10
❖ MPTP + PF-475 10 mg/kg n=10

ENDPONTS	
Brain	Colon
• PD hallmarks • Mitophagy pathway	• Histopathological evaluation • Inflammatory markers • -synuclein accumulation • Enteric nervous system markers • Mitophagy pathway • Tight junction proteins

Experimental timeline

Study design of *in vivo* experiment.

Experimental groups and procedure of the study

Experimental Groups		Experimental Procedure	N°
1)	CONTROL	Vehicle solution (saline) was injected intraperitoneally for 7 consecutive days	10

(*Continued on next page*)

Continued

Experimental Groups		Experimental Procedure	N°
2)	CONTROL +PF-475 2.5 mg/kg	PF-475 2.5 mg/kg was administered intraperitoneally for 7 consecutive days starting 24 h after vehicle solution injection	10
3)	CONTROL + PF-475 5 mg/kg	PF-475 5 mg/kg was administered intraperitoneally for 7 consecutive days starting 24 h after vehicle solution injection	10
4)	CONTROL + PF-475 10 mg/kg	PF-475 10 mg/kg was administered intraperitoneally for 7 consecutive days starting 24 h after vehicle solution injection	10
5)	MPTP	MPTP solution was administered intraperitoneally during the first day, and saline intraperitoneal administration for 7 consecutive days starting 24 h after MPTP injection.	10
6)	MPTP + PF-475 2.5 mg/kg	MPTP solution was administered intraperitoneally during the first day, and PF-475 2.5 mg/kg intraperitoneal administration for 7 consecutive days starting 24 h after MPTP injection.	10
7)	MPTP + PF-475 5 mg/kg	MPTP solution was administered intraperitoneally during the first day, and PF-475 5 mg/kg intraperitoneal administration for 7 consecutive days starting 24 h after MPTP injection.	10
8)	MPTP + PF-475 10 mg/kg	MPTP solution was administered intraperitoneally during the first day, and PF-475 10 mg/kg intraperitoneal administration for 7 consecutive days starting 24 h after MPTP injection.	10

Recent studies have confirmed MPTP-induced PD animal models as a validated method to study PD-related disorders of the intestinal environment.[37,62,63] Indeed, MPTP neurotoxin in mice increases colonic motility associated with dopaminergic degeneration in the ENS and increases alpha-synuclein, which has been identified in the colon of PD patients. Compared to other neurotoxins, MPTP is a dopaminergic neuronal toxin selective in ENS changes that alters colonic motility. Furthermore, numerous studies demonstrated that MPTP is a useful neurotoxin for exploring the pathophysiological basis of gastrointestinal dysmotility in PD and to develop an animal model in which to study the debilitating gastrointestinal symptoms associated with PD.[32,33,64] The PF-475 route and doses of administration was based on previous *in vivo* study.[14] The minimum number of mice for every technique was estimated with the statistical test "ANOVA: Fixed effect, omnibus one-way" with G-power software. The G* power analysis produced a minimum total number of mice of 80 which, when divided into the 8 groups, leads to an effective sample size of 10 mice/group. Therefore, 10 mice were enrolled for histological analyzes (histology, immunohistochemistry, and immunofluorescence), 10 mice for western blot and ELISA analyses, and 10 mice for high-performance liquid chromatography (HPLC). Animals were monitored daily for morbidity and mortality, and their body weight was monitored weekly to assess overall health. At the end of the experiment the survival rate was 100%. Data regarding control mice subjected to intraperitoneally treatment with PF-475 at different doses (2.5, 5 and 10 mg/kg) are not shown because of no significant changes reported in control + PF-475 2.5, 5 and 10 mg/kg treated mice compared to the control + vehicle mice.

Experimental groups

Animals were randomly divided as summarized in the table in the "induction of MPTP mouse model" section.

Western blot analysis

For western blot analysis, the brain and colon tissues were surgically isolated. Tissue samples were processed and were suspended in two different buffers (buffer A and B) to extract the cytosolic and nuclear fractions. Buffer A contains 0.2 mM PMSF, 0.15 mM pepstatin A, 20 mM leupeptin, and 1 mM sodium orthovanadate. Subsequently, samples homogenized with buffer A were centrifuged at 12,000 rpm for 4 min at 4°C. The supernatants obtained represented the cytosolic portion, the pellets instead represent the nuclear part. Immediately after, the pellets were suspended in buffer B and centrifuged for 10 min at 4°C, and the supernatants part was collected and stored at −20°C for further analysis. Buffer B contains 1% Triton X-100, 150 mM NaCl, 10 mM Tris–HCl pH 7.4, 1 mM EGTA, 1 mM EDTA, 0.2 mM PMSF,

20 mM leupeptin, 0.2 mM sodium orthovanadate.[14,65] The expression of leucine-rich repeat kinase 2 (LRRK2), phosphorylated LRRK2 at Serine935 (p-Ser935), cyclooxygenase-2 (COX-2), inducible nitric oxide synthase (iNOS), α-Synuclein, protein gene product 9.5 (PGP9.5), neuron specific enolase (NSE), ubiquitin-binding protein p62 (p62), optineurin (OPT), lysosome-associated membrane protein-2 (LAMP2) , and tumor necrosis factor- α (TNF- α) were quantified in cytosolic proteins fractions. Protein samples were used for the SDS page, subsequently, membranes were incubated overnight with the following primary antibodies: the following primary antibodies diluted in milk, Phospahate-Buffered Saline (PBS), and 0.1% Tween-20 (PMT): anti-LRRK2 (1:1000 Abcam, ab-133474), anti-phosphorylated LRRK2 at Serine935 (1:1000 Abcam, ab-133450) anti-iNOS (1:500; Santa Cruz Biotechnology, Dallas, TX, USA; sc-7271); anti-COX2 (1:500; Santa Cruz Biotechnology, Dallas, TX, USA; sc-376861), anti-α-Synuclein (1:500; Santa Cruz Biotechnology, Dallas, TX, USA; sc-7011), anti-PGP9.5 (1:1000; Elabscience, Cat no. E-AB-53097); anti-NSE (1:1000; Invitrogen, PA5-94940); anti-p-62 (1:1000, Abcam, ab91526), anti-optineurin (1:500; Santa Cruz Biotechnology, Dallas, TX, USA; sc-166576); anti-LAMP2 (1:1000; Invitrogen, MA1-205); anti-TNF-α (1:500; Santa Cruz Biotechnology sc-52746); anti-p-Rab12 (1:500; ab256487, Abcam); anti-Rab12 (1:500, 18843-1-AP, Proteintech); anti-p-Rab10 (1:500 ab230261, Abcam); anti-Rab10 (1:500, ab104859, Abcam); anti-Occludin (1:500; Santa Cruz Biotechnology, Dallas, TX, USA; sc-133256), anti-ZO-1 (1:500; Santa Cruz Biotechnology, Dallas, TX, USA; sc-33725). To confirm that the samples contained an equal protein concentration, membranes were incubated with primary anti-β-actin antibody (1:500; sc-47778; Santa Cruz Biotechnology, Dallas, TX, USA). Finally, signals were revealed by enhanced chemiluminescence (ECL) detection system reagent according to the manufacturer's instructions (SuperSignal West Pico Chemiluminescent Substrate, Thermo Fisher Scientific, Waltham, MA, USA). The relative expression of the protein bands was quantified by densitometry with BIORAD ChemiDoc™XRS + software and standardized to β-actin levels as internal control.

Measurement of dopamine, 3,4-dihydroxyphenylacetic acid (DOPAC), and homovanilic acid (HVA) levels in the striatum

Dopamine and its metabolites, 3,4-dihydroxyphenylacetic acid (DOPAC) and homovanilic acid (HVA) were quantified via high performance liquid chromatography (HPLC) with electrochemical detection, using 0.15 M monochloroacetic acid, pH 3.0, and 200 mg/L sodium octyl sulfate, 0.1 mM EDTA, 4% acetonitrile, and 2 .5% tetrahydrofuran as mobile phase. Data were collected and processed on a Dynamax (Rainin Instruments) computerized data manager.[66]

Enzyme-linked immunosorbent assay (ELISA kit)

The ELISA kit assay was performed on the protein extract of colon samples to determine the concentration of proinflammatory cytokine IL-1β according to manufacturer' instructions (Mouse IL-1β ELISA Kit, Abcam, ab197742).

Histological evaluation

Histological analyses were performed to assess colonic morphological changes.[67] Briefly, after the sacrifice, colon tissues were fixed in 10% (w/v) PBS-buffered formaldehyde solution at 25°C for 24 h. After a dehydration process through a scale of increasing concentrations of alcohols and xylene, tissues were included in paraffin (Bio-Optica, Milan, Italy) and subsequently cut under the microtome obtaining 7 μm thick sections. For morphological analyses, slides were stained with Hematoxylin/Eosin (H&E, Bio-Optica, Milan, Italy) to assess histological alterations, edema, and neutrophilic infiltration. We used the following morphologic criteria for the histological analysis: score 0 no morphologic damage; score 1 focal epithelial edema as well as necrosis; score 2 diffuse inflammation and necrosis of villous area; score 3 presences of neutrophilic infiltration in submucosa area; score 4 necrosis and neutrophil infiltration; score 5 massive neutrophilic infiltration. All sections were examined at an objective lens of 20x and 40x by using a Nikon Eclipse Ci-L microscope.

Immunohistochemistry analysis

At the end of the experiment, the presence of PGP9.5 marker and α-synuclein in colon tissues, was investi-gated by immunohistochemistry.[68] Colon samples were immediately fixed in 10% (w/v) PBS-buffered formaldehyde solution at 25°C for 24 h. After a dehydration process through a scale of increasing concentrations of alcohols and xylene, tissues were included in paraffin (Bio-Optica, Milan, Italy) and subsequently cut with microtome into 7 μm slices and, after deparaffinization, endogenous peroxidase was quenched with 0.3% (v/v) hydrogen peroxide in 60% (v/v) methanol for 30 min. Slides were permeabilized with 0.1% (w/v) Triton X-100 in PBS for 20 min. Non-specific adsorption was decreased by incubating the section in 2% (v/v) normal goat serum in PBS for 20 min. Endogenous avidin or biotin binding sites were blocked by sequential incubation for 15 min with avidin and biotin (Vector Laboratories, Burlingame, CA, USA), respectively. Then, sections were incubated overnight (O/N) with the following primary antibodies: anti-PGP9.5 (Elabscience, Cat no. E-AB-53097) and α-synuclein (1:100; sc-7011; Santa Cruz Biotechnology, Dallas, TX, USA). Then, the sections were washed with PBS and incubated with secondary antibody for 1 h. The reaction was revealed using the water-soluble, chromogenic substrate 3,3′-Diaminobenzidine (DAB), and counter-stained with Nuclear Fast Red. The percentage area of immunoreactivity (determined by the number of positive pixels) was expressed as the % of total tissue area (red staining) within five random fields at an objective lens of 40 × and analyzed using a computerized image analysis system (Leica QWin V3, Cambridge, UK). All stained sections were observed and analyzed in a blinded manner at an objective lens of 20x and 40x by using a Nikon Eclipse Ci-L microscope.

Immunofluorescence analysis

After deparaffinization and rehydration, detection of ZO-1 and Occludin was performed after heating the colon sections in 0.1 M citrate buffer for 1 minute. Non-specific adsorption was diminished by incubating the section in 2% (vol/vol) bovine serum albumin in PBS for 20 min.[68] Sections were incubated with anti-ZO-1 (1:100; Santa Cruz Biotechnology, Dallas, TX, USA; sc-33725) or anti-occludin (1:100; Santa Cruz Biotechnology, Dallas, TX, USA; sc-133256) antibodies in an O/N humidified chamber. The sections were then incubated with a secondary antibody, a fluorescein-isothiocyanate (FITC) conjugated anti-mouse Alexa Fluor-488 antibody (1:1000 v/v Molecular Probes, Altrincham, UK), for 3 hours at room temperature. Finally, after washing with PBS, nuclei were stained by adding 2 μg/mL 40,60-diamidino-2-phenylindole (DAPI; Hoechst, Frankfurt, Germany). Sections were observed at an objective lens of 40x by using a Nikon Eclipse Ci-L microscope. using a Nikon Eclipse Ci-L microscope. For each antibody analyzed, positive cells were counted stereologically on the sections by examining the most brightly labeled pixels and applying settings that allowed clear visualization of structural details. The same settings were used for all images obtained from the other samples which were processed in parallel.

Determination of fecal weight

Determination of fecal weight was performed as constipation-related indicator.[69] Fecal weight was measured every day from day one to day seven.

Adenosine triphosphate (ATP) assay

Mitochondrial function was assessed by measuring ATP levels. ATP levels were measured from brain and colon protein samples using a standard curve method by using ATP ELISA kit (MyBiosource Cat No. MBS267352), according to the manufacturer's instructions. The plate was read in an microplate reader with an absorbance wavelength of 450 nm.[25]

Malondialdehyde (MDA) assay

Malondialdehyde (MDA), a byproduct of lipid peroxidation, has been established to assay mitochondrial activity.[70] Brain and colon tissues were homogenised in 1.15% (w/v) KCl solution. A 100 μl aliquot of the homogenate was added to a reaction mixture containing 200 μl of 8.1% (w/v) SDS, 1.5 ml of 20% (v/v) acetic acid (pH 3.5), 1.5 ml of 0.8% (w/v) thiobarbituric acid and 700 μl distilled water. Samples were then boiled for 1 h and centrifuged for 10 min. The absorbance of the supernatant was measured using spectrophotometry at 650 nm.[67,71]

QUANTIFICATION AND STATISTICAL ANALYSIS

Values are means ± SD. Distribution of values come from individual animals. The results were analyzed with GraphPad 9 software by one-way analysis of variance (ANOVA), followed by a Bonferroni post hoc test for multiple comparisons. A p-value of less than 0.05 was considered significant.